2009

On Active Disturbance Rejection Control;Stability Analysis and Applications in Disturbance Decoupling Control

Qing Zheng
Cleveland State University

ON ACTIVE DISTURBANCE REJECTION CONTROL: STABILITY ANALYSIS AND APPLICATIONS IN DISTURBANCE DECOUPLING CONTROL

QING ZHENG

Bachelor of Science in Electrical Engineering

North China University of Technology

July, 1996

Master of Engineering in Electrical Engineering

National University of Singapore

July, 2003

submitted in partial fulfillment of the requirements for the degree

DOCTOR OF ENGINEERING

at the

CLEVELAND STATE UNIVERSITY

July 2009

This dissertation has been approved for the

Department of **ELECTRICAL AND COMPUTER ENGINEERING**

and the College of Graduate Studies by

_____

Dissertation Committee Chairperson, Dr. Zhiqiang Gao

_____

Department/Date

_____

Dr. Lili Dong

_____

Department/Date

_____

Dr. Paul Lin

_____

Department/Date

_____

Dr. Sally Shao

_____

Department/Date

_____

Dr. Dan Simon

_____

Department/Date

_____

Dr. Sridhar Ungarala

_____

Department/Date

To my family...

It is their anticipation that stimulates me to pursue a high education!

ACKNOWLEDGMENTS

I would like to express my most sincere gratitude to my advisor, Dr. Zhiqiang Gao, for his consistent guidance, patience, and support during the whole period of my study. Dr. Gao's rigorous scientific approach and endless enthusiasm in research have influenced me greatly. His erudite knowledge as well as deep insights in the field of control make this research an invaluable experience. Without his stimulating discussions and continuous encouragement, this dissertation and many other results would have been impossible.

Special thanks go to Dr. Lili Dong, Dr. Paul Lin, Dr. Sally Shao, Dr. Dan Simon, and Dr. Sridhar Ungarala, who are on my dissertation committee, for their time in reviewing and evaluating this dissertation as well as for their guidance on my research.

I am also thankful for the peer advice from my lab partners, especially Gang Tian, Shen Zhao, Jeff Csank, Classica Jain, and Zhongzhou Chen, but also including Frank Goforth, Aaron Radke, Rob Miklosovic, Wankun Zhou, David Avanesov, and Dae Hui Lee.

In this dissertation, Some sections of some chapters are reprinted from my earlier publications during my doctoral study, with the permission from IEEE. Thank IEEE for granting this permission.

My deepest gratitude is due to my family members. Without their love, patience, encouragement, and sacrifice, I would not have accomplished this. I wish to dedicate this dissertation to all of them.

ON ACTIVE DISTURBANCE REJECTION CONTROL: STABILITY ANALYSIS AND APPLICATIONS IN DISTURBANCE DECOUPLING CONTROL

QING ZHENG

ABSTRACT

One main contribution of this dissertation is to analyze the stability characteristics of extended state observer (ESO) and active disturbance rejection control (ADRC). In particular, asymptotic stability of the dynamic system that describes the estimation error and the closed-loop system is established where the plant dynamics is completely known. In the face of large dynamic uncertainties, the estimation error, the closed-loop tracking error, and its up to the $(n-1)^{st}$ order derivatives are shown to be bounded. Furthermore, it is demonstrated that the error upper bounds, in general, monotonously decrease with the observer and control loop bandwidths. The second contribution is to develop a dynamic disturbance decoupling control strategy for square multivariable systems based on ADRC. The proposed method has been successfully applied to chemical process problems and micro-electro-mechanical systems gyroscopes. It is shown that a largely unknown square multivariable system can be readily decoupled by actively estimating and rejecting the effects of both the internal plant dynamics and external disturbances. By requiring little information on the plant model, the intention is to make the new decoupling approach practical.

TABLE OF CONTENTS

LIST OF TABLES

LIST OF FIGURES

ACRONYMS

UIO unknown input observer

DOB disturbance observer

POB perturbation observer

ESO extended state observer

ADRC active disturbance rejection control

MIMO multiple-input multiple-output

MEMS micro-electro-mechanical systems

SISO single-input single-output

PID proportional, integral, and derivative

FLC fuzzy logic control

ANN artificial neural network

GD generalized disturbance

HGO high gain observer

ECP Educational Control Products

CSTR continuous stirred tank reactor

MPC model predictive control

LPF low pass filter

CHAPTER I

INTRODUCTION

Most existing control design methods, such as Bode plot method in classical control and H_2/H_∞ control in modern control theory, are based on mathematical description of plant dynamics. However, many physical plants in real world are not only nonlinear and time-varying but also highly uncertain. Accurate mathematical descriptions of physical plants are usually not available in industrial control. This creates a dilemma for control practitioners: the requirement of the plant mathematical model from the theoretical side and the uncertainty of the plant dynamics in practice. Such dilemma caught much attention of many researchers. One solution is robust control, where a small amount of uncertainty in physical plants can be tolerated.

Another dilemma in control system design is how to handle disturbances. In the current modern control framework, disturbance attenuation is one of key control design objectives. A less known solution is to estimate and cancel disturbance directly. To this end, many disturbance estimators, such as unknown input observer (UIO) [1]-[8], disturbance observer (DOB) [9]-[16], perturbation observer (POB) [17]-[20], and extended state observer (ESO) [21]-[27], have been proposed. Based on the ESO,

an active disturbance rejection control (ADRC) algorithm has also been developed [21]-[27]. The ADRC offers a new and inherently robust controller building block that requires very little information of the plant. This control algorithm actively estimates and compensates for the effects of the unknown dynamics and disturbances, forcing an otherwise unknown plant to behave like a nominal one. Such strategy offers an alternative to the prevailing methods. That is, instead of depending on the model of the plant, the controller draws the information needed from the ESO to control the plant. This is achieved by using an ESO to estimate both internal plant dynamics and external disturbances.

In robust control, the stability analysis is mostly based on the small gain theorem, and the results tend to be quite conservative by nature. As to the class of disturbance estimators UIO, DOB, and POB, the rigorous stability proof or convergence is not established, although a few researchers speculated this could be done. Although the ESO and the ADRC have been applied to solve many different kinds of problems, their convergence and stability have not been proven. Furthermore, there is a lack of understanding of the exact relationship between the control system tuning parameters and the performance requirements. In short, we know the ADRC works, but do not know why. In particular, the relationship between the tuning parameters, which include the observer and controller bandwidths, and the observer estimation error and the closed-loop tracking error is unknown. Without rigorous analytical study, the ADRC remains a trial and error method. Therefore the stability and convergence analysis for the ESO and the ADRC is essential.

In this dissertation, one key objective is to provide an analytical insight on why ADRC achieves excellent performance, that is, to mathematically show that both the external disturbance and the plant dynamics can be estimated by ESO. Estimating the unknown parameters in plants has been studied in system identification. Estimating

both the external disturbance and the plant dynamics crosses the boundary between system identification and observer design. Whether the combined effect of plant dynamics and external disturbance can be estimated in real time or not is of great importance, because if the answer is yes, it could mean that the uncertainty problem, the adaptive control problem, and disturbance rejection problem, can all be handled in one single framework.

The mathematical proof of the ESO convergence and the ADRC stability renders the theoretical support of why the ADRC can achieve high disturbance rejection and robustness performance. It also explains why the ADRC has been successfully applied to many applications. In this dissertation, the ADRC is extended to another important class of practical problems, namely the decoupling control for multivariable systems.

The interactions or cross-couplings between the variables are the most significant characteristics with multivariable systems, i.e., systems with multiple inputs and multiple outputs, also known as multiple-input multiple-output (MIMO) systems. With the interactions or cross-couplings present, one input variable may affect all the output variables. In a vibrational micro-electro-mechanical systems (MEMS) gyroscope [28], the quadrature error is caused by coupling in the stiffness term between its drive and sense axes. In the Wood and Berry column example [29], the inputs reflux and vapor flow both affect the two outputs, which are the top and bottom composition. The interactions or cross-couplings among various inputs and outputs of a system make design technologies in multivariable control systems fundamentally different from single-input single-output (SISO) control systems. Given that our understanding of the physics of MIMO systems usually helps us identify the dominant input-output pairs, one design strategy is to disentangle the interactions among various input-output pairs and reduce a multivariable system into a number

of independent SISO systems. This strategy is usually known as decoupling.

Although the interactions are present in most multivariable systems, the control engineers in industry frequently ignore the interactions between variables and design the controller for each loop independently. In most cases, proportional, integral, and derivative (PID) control is preferred. This is not because the control engineers are not aware of the interactions but because the existing methods for solving the problem are difficult for engineers to understand and implement, either due to their mathematical complexity or due to the unavailability of the necessary model information. Therefore, it is important to find an approach that can address the interaction problems and is practical and easy to be implemented in industry. This leads to the second key objective of this research, that is, to develop a new practical decoupling control approach for multivariable systems.

In this dissertation, we first analyze the stability characteristics of the ESO and the associated ADRC, then discuss the proposed disturbance decoupling control (DDC) approach. The organization of the dissertation is as follows. The stability problem of the ADRC and the decoupling problem are formulated in Chapter 2, where the literature survey for disturbance estimators, stability analysis of disturbance estimators, and decoupling control is also given. The idea of the ADRC is introduced and its effectiveness is demonstrated through simulation and hardware tests in Chapter 3. The stability characteristics for the ESO and the ADRC are analyzed in Chapter 4. A novel and practical DDC approach is proposed in Chapter 5. Simulation results obtained on two chemical process problems are shown in Chapter 6. The applications of DDC to MEMS gyroscopes are performed in Chapter 7. Finally, the highlight of the major contributions of this dissertation and the recommendations on possible future research directions that may be pursued based on the insights gained from this research are given in Chapter 8.

CHAPTER II

PROBLEM FORMULATION AND LITERATURE SURVEY

This chapter begins with problem formulation of the ADRC stability analysis and decoupling control, followed by a literature survey on disturbance estimation, stability analysis of disturbance estimators, and decoupling control.

2.1 Problem Formulation

This section discusses what is the problem of the ADRC stability characteristics and why a new decoupling control is needed.

2.1.1 The Problem of ADRC Stability Characteristics

Most physical plants in real world are not just nonlinear and time-varying but also highly uncertain. Control system design for such systems has been the focus of much of the recent developments under the umbrella of robust, adaptive, and nonlinear control. Most of the existing results, however, are obtained presupposing that

a fairly detailed and accurate mathematical model of the plant is available. The small gain theorem based robustness analysis does allow a small amount of uncertainties in plant dynamics, but not anywhere near the magnitude often encountered in practice. As the well-known control theorist Roger Brockett puts it: "If there is no uncertainty in the system, the control, or the environment, feedback control is largely unnecessary" [30]. The assumption that a physical plant, without feedback, behaves rather closely as its mathematical model describes, as the point of departure in control system design, does not reflect either the intent of feedback control, or the physical reality.

The ADRC was proposed as an alternative paradigm to address this fundamental issue [21]. The main difference in the design concept pertains to the question of how much model information is needed. Recognizing the vulnerability of the reliance on accurate mathematical model, there has been a gradual recognition over the years that active disturbance estimation is a viable alternative to an accurate plant model. That is, if the disturbance, representing the discrepancy between the plant and its model, is estimated in real time, then the plant-model mismatch can be effectively compensated for, making the model based design tolerant of a large amount of uncertainties. The focal point is how external disturbance and unknown dynamics can be estimated.

The ADRC is designed to deal with those plants with large amount of uncertainties both in dynamics and external disturbances [22]-[26]. It was further simplified to linear ADRC, using linear ESO in [27], which makes it extremely simple and practical [31]-[32]. Although the ADRC has a wide variety of applications, the stability analysis of the ADRC is scarce in literature. We know the ADRC works, but do not know why. Furthermore, there is a lack of understanding of the exact relationship between the control system tuning parameters and the performance requirements.

Without rigorous analytical study, the ADRC remains a trial and error method. This dissertation specifically addresses these issues. Through analyzing stability characteristics of the ADRC, we want to understand why the ADRC works, i.e., what is the stability characteristics of the ADRC; and how to tune it, i.e, whether there is a relationship between the performance of the ADRC and the bandwidths of the observer and the controller.

2.1.2 The Disturbance Decoupling Control Problem

The decoupling problem for systems with large uncertainties of the internal dynamics and significant unknown external disturbances is very challenging.

Consider a multivariable system

$$\begin{bmatrix} y_1(s) \\ y_2(s) \\ \vdots \\ y_m(s) \end{bmatrix} = \begin{bmatrix} g_{11}(s) & g_{12}(s) & \cdots & g_{1m}(s) \\ g_{21}(s) & g_{22}(s) & \cdots & g_{2m}(s) \\ \vdots & \vdots & \ddots & \vdots \\ g_{m1}(s) & g_{m2}(s) & \cdots & g_{mm}(s) \end{bmatrix} \begin{bmatrix} u_1(s) \\ u_2(s) \\ \vdots \\ u_m(s) \end{bmatrix}, \tag{2.1}$$

with the mathematical model, it can be decoupled to the following system

$$\begin{bmatrix} y_1(s) \\ y_2(s) \\ \vdots \\ y_m(s) \end{bmatrix} = \begin{bmatrix} G_{11}(s) & 0 & \cdots & 0 \\ 0 & G_{22}(s) & \cdots & 0 \\ \vdots & \vdots & \ddots & \vdots \\ 0 & 0 & \cdots & G_{mm}(s) \end{bmatrix} \begin{bmatrix} u_1(s) \\ u_2(s) \\ \vdots \\ u_m(s) \end{bmatrix}. \tag{2.2}$$

Since the mathematical model is often unavailable in practice, sometimes it is impossible to obtain the mathematically decoupled form of the system as shown in (2.2). The question is: can we make the system behave as a decoupled system without a mathematical model? In other words, without using the mathematical model to get the mathematical description of the decoupled form for a system, can we make it really operate as a decoupled system?

More generally, Let

$$\begin{aligned}
\vartheta_1 &= \left[y_1^{(n_1-1)}(t), y_1^{(n_1-2)}(t), \cdots, y_1(t)\right], \\
\vartheta_2 &= \left[y_2^{(n_2-1)}(t), y_2^{(n_2-2)}(t), \cdots, y_2(t)\right], \\
&\vdots \\
\vartheta_m &= \left[y_m^{(n_m-1)}(t), y_m^{(n_m-2)}(t), \cdots, y_m(t)\right], \\
u &= \left[u_1(t), u_2(t), \cdots, u_m(t)\right], \\
w &= \left[w_1(t), w_2(t), \cdots, w_m(t)\right].
\end{aligned} \tag{2.3}$$

where y_i is the output, u_i is the input, w_i is the external disturbance of the i^{th} loop, $y_i^{(n_i)}$ denotes the n_i^{th} order derivative of $y_i, i = 1, 2, \cdots, m$, and f_i represents the combined effect of internal dynamics and external disturbance in the i^{th} loop, including the cross channel interference. Consider the following nonlinear time varying system with unknown dynamics

$$\begin{aligned}
y_1^{(n_1)} &= f_1(\vartheta_1, \vartheta_2, \cdots, \vartheta_m, u, w) + b_{11}u_1 \\
y_2^{(n_2)} &= f_2(\vartheta_1, \vartheta_2, \cdots, \vartheta_m, u, w) + b_{22}u_2 \\
&\vdots \\
y_m^{(n_m)} &= f_m(\vartheta_1, \vartheta_2, \cdots, \vartheta_m, u, w) + b_{mm}u_m
\end{aligned} \tag{2.4}$$

Note that $i = 1, 2, \cdots, m$.

Without a mathematical model, can we design a control strategy to stabilize the system and make it run as a decoupled system? Can we find a new alternative to the existing decoupling approaches, which are based on the mathematical description of the plant? The new alternative should be conceptually simple and easy to understand, and above all, practical to implement, for real world decoupling problems, in the presence of significant unknown disturbances and unmodeled dynamics.

In this dissertation, we seek a novel and practical approach to DDC that requires very little information of the plant dynamics.

2.2 Literature Review

In this section, an extensive literature review for disturbance estimator, stability analysis of disturbance rejection, and decoupling is conducted.

2.2.1 A Survey of Disturbance Estimation

State observers, also known as estimators, play a central role in modern control theory. Given the input-output data, the values of internal variables of a physical plant,which are often inaccessible instrumentation wise, are made available through state observers. Such information extracted by the state observers proved to be invaluable in control system design, as well as fault detections . Please refer to recent surveys [33, 34].

A presumption in most existing state observer design is that an accurate mathematical model of the plant has been obtained. While this is a common assumption made in academia, it could pose some rather considerable challenges time and cost wise in engineering practice. The sometimes prohibitive cost and limitation associated with obtaining a good mathematical model drove a significant number of researchers and engineers to seek alternatives, such as fuzzy logic control (FLC) and artificial neural network (ANN), but there is more than an inconvenience at stake here. If the primary purpose of employing feedback control is to counter the uncertainties in physical devices so that a precise and consistent behavior can be obtained from a system that consists of devices with inconsistent and only partially known dynamics, why does most of the modern control theory insist on having a precise mathematical model prior to any analysis and design?

The everyday users of feedback control, however, are concerned about if there is a viable alternative, an alternative that does not completely abandon most advances made in modern control theory, as in the case of FLC and ANN, but does away

with the obsession with mathematical model. Some researchers over the years have investigated the problem of real time estimation of the disturbance, i.e. the part of the plant that is not described by the mathematical model. The ingenious idea is that if such discrepancy between the plant and its model can be computed and compensated for in real time, the closed-loop system behavior will not be hinged upon the accuracy of the plant model.

One class of such disturbance estimators is the UIO [1]-[8], where the disturbance is treated as an augmented state of the plant. The state observer is designed to estimate both the original states and the augmented one. The disturbance is then rejected by using its estimated value obtained by the observer. Another class of disturbance estimators is known as the DOB [9]-[16], where the disturbance is estimated by using the inverse of the nominal transfer function of the plant. In addition to the UIO and the DOB, there are also scattered reports of different variations, such as the adaptive robust controller, the adaptive inverse controller, and model-based disturbance attenuation method. Some researchers proposed the POB [17]-[20] to estimate the disturbances in a discrete state space form.

Another important class of such disturbance estimators is the ESO [21]-[27]. The ESO is a state space approach. What sets the ESO apart from the UIO and the DOB is that it is conceived to estimate not only external disturbances but also plant dynamics. Among the disturbance estimators, the ESO requires the least amount of plant information. As one class of such disturbance estimators, the ESO was first proposed by Han in the context of the ADRC [22]-[25]. The ADRC as a new design paradigm was first introduced to the English literature in [26]. The ADRC using nonlinear gains was successfully applied to a complex Stewart platform control problem in [31]. Although the idea is quite imaginative, the nonlinear structure and a large number of tuning parameters, which need to be manually adjusted in

implementation, make its large scale practical applications challenging. Central to this novel design framework is the ability to estimate generalized disturbance (GD) in real time.

The estimation of both unknown dynamics and disturbance has been studied in [35], but it requires the higher order derivatives of the output, which may not be available in practice. The estimation of unknown dynamics can also be achieved by the high gain observer (HGO) [36]-[39], however, the high gain associated with the HGO makes the system too sensitive to noise.

2.2.2 A Survey of Stability Analysis of Disturbance Estimators

All estimators above, including the UIO, the DOB, and the POB, prove to be effective practical solutions. But how fast and in what range the disturbance and unknown dynamics can be estimated are not obvious. In particular, both the UIO and the DOB are originally formulated to estimate the external disturbances but later adopted to estimate the unknown plant dynamics as well, with very little analytical support on how this can be achieved. Even when limited stability analysis was performed, only boundedness of estimation or compensation error was obtained, while the actual bound of the error is largely unknown. Some robust stability analysis, based on small gain theorem, was performed for the UIO and the DOB [14]-[16] but the results tend to be quite conservative by nature and limited to linear and time-invariant plants. For nonlinear plants, only limited results on stability properties are obtained for robot manipulators [10], [13].

In a rare exception, the approach proposed by [35] is designed specifically to estimate both unknown dynamics and disturbance with asymptotic stability of the closed-loop system firmly established. But the practicality method is quickly called

into question as the observer, hence the stability proof, requires the use of higher order derivatives of the output, rendering the system susceptible to noise corruption. In short, for those effective practical solutions, there seems to be a lack of rigorous analysis of the estimation error, especially its bound. But for those methods firmly rooted in mathematical rigor, the utility is often questionable.

The ESO and the associated ADRC can effectively estimate not only external disturbances but also plant dynamics. In addition, the ADRC has been widely used in various problems [32]-[43]. A singular perturbation approach is used to show there exists a small gain to guarantee that the origin of the error dynamics is exponentially stable under strict assumptions [44]. However, the error upper bound and its relationship to the bandwidth are not given, which are the concerns of this dissertation.

As to the HGO, in fact, there is a marked similarity between the HGO and the ESO in terms of how the observer gains are selected, leading some readers to suspect that the ESO is a special case of the HGO. To clarify this issue, the difference between the HGO and the ESO is seen in the following four aspects. 1). The plant and problem formulation are very different. With the HGO, the task is to estimate the states for a class of nonlinear plants as $y^{(n)} = f(\cdot) + g(\cdot)u^{(m)}$, with a nominal model of $f_0(\cdot)$ and $g_0(\cdot)$. On the other hand, in addition to the state estimation, the ESO is specifically designed to estimate the effects of unknown dynamics and external disturbances for a different class of plants, mostly unknown, nonlinear and time-varying: $y^{(n)}(t) = f\left(y^{(n-1)}(t), y^{(n-2)}(t), \cdots, y(t), w(t)\right) + bu(t) = F(t) + bu(t)$, where w is an external disturbance and $F(t) = f\left(y^{(n-1)}(t), y^{(n-2)}(t), \cdots, y(t), w(t)\right)$ is to be estimated as an extended state. With $f(\cdot)$ as a mathematical expression completely unknown, the ADRC is a novel design methodology by which $f(\cdot)$ is treated as a variable to be estimated and canceled in the control law, thus making

the design largely model independent. 2). The goal and approach used in stability analysis are different. In the HGO, Lyapunov method and singular perturbation are used to derive stability conditions. In the ADRC analysis, we seek the insight on the relationship between the tracking error and the bandwidth, which helps to guide the users in tuning the feedback system in real world applications. In fact, we were able to show, by solving the differential equation of error dynamics, that the estimation error is bounded and, more importantly, monotonously decreases with the observer bandwidth. 3). The assumptions made in the HGO and the ESO are different. The analysis of the HGO is predicated on six different mathematical assumptions that are, though convenient, not necessarily easy to verify in a given physical process. The only assumption in the ESO is that $h = \dot{f}$ is bounded and this, we believe, agrees with most physical systems where the rate of change associated with the highest derivative is physically limited. For example, the jerk generated by a DC motor can be unknown but it is limited by the supply voltage. On the other hand, the assumption that $f(\cdot)$ is Lipschitz in [37] is not necessary in our framework, nor is it valid in the presence of certain external disturbance, such as a ramp disturbance. 4). The conclusions of the HGO and the ESO are different. For the HGO, based on six assumptions, it is shown the state, in its common definition, can be estimated where the tracking error can be made arbitrarily small with the increasing observer gains. With the ESO, we show that not only the state but also the unknown plant dynamics and disturbance, namely $F(t) = f\left(y^{(n-1)}(t), y^{(n-2)}(t), \cdots, y(t), w(t)\right)$, can be estimated with a bounded error. This has simply not been done before and it has enormous practical implications.

2.2.3 A Survey of Decoupling Control

Decoupling of linear time invariant (LTI) multivariable systems has drawn researchers' interest in the past several decades [45]-[73], making it a well established

area. The long research records on decoupling control reveal that this topic has now been well studied, at least for the systems with parameters being exactly known. In sharp contrast to other issues of control theory, the study of decoupling problem for uncertain systems has rarely been reported in the literature. This phenomena is unsatisfactory since parameter perturbation or deviation from their nominal values is inevitable in real plants, especially in industrial process control. Intuitively, strict decoupling is very difficult to achieve due to the presence of plant parameter perturbations. In practice, it is often the case that first design a decoupling controller (decoupler) for the nominal model of the real plant, put the decoupler as the inner loop controller and then on-line tune the outer loop controller to make the overall system performance be roughly satisfied. Reference [74] describes such a procedure. In robot control systems, the calculated torque method combined with gain scheduling also belongs to this approach [75].

Among the many existing decoupling methods, their mathematical complexity or requirements of the specific model information prevent them from prevailing in industry. Robustness, disturbance rejection, and other practical concerns continue to pose serious challenges [45]. In conjunction with decoupling control, the importance of disturbance rejection has been recognized by many researchers. One main stream of disturbance rejection methods for decoupling control is based on the concept of the disturbance estimation, which was outlined in Section 2.2.1. The effectiveness of the existing disturbance rejection methods, such as the UIO, the DOB, and the POB, is limited by the requirement of an accurate mathematical model of the plant. In engineering practice, however, such presumption is hardly warranted as many industrial processes are highly uncertain and are in a perpetual flux. This also explains why currently PID control is still very popular and is the most commonly used control method in practice. It is one target of this research to find a new alternative that is

conceptually simple and easy to understand, and above all, practical to implement, for real world decoupling problems, in the presence of significant unknown disturbances and unmodeled dynamics.

2.3 Summary

Chapter 2 formulates the problems that this dissertation addresses and presents a literature review on disturbance estimation, stability analysis of disturbance estimators, and decoupling control. The problem formulation and the literature survey show that the proposed research in this dissertation is indeed meaningful.

CHAPTER III

ACTIVE DISTURBANCE REJECTION CONTROL

The ADRC is a quite different design philosophy. At its foundation is the recognition that, in the real world, dynamic systems are often highly uncertain, both in terms of the internal dynamics and external disturbances. The magnitude of the uncertainties could make them well beyond the reach of prevailing robust control theories, such as H_2/H_∞. The ADRC offers a solution where the necessary modeling information needed for the feedback control system to function well is obtained through the input-output data of the plant in real time. Consequently, the control system can react promptly to the changes either in the internal dynamics of the plant, or its external disturbances. In the ADRC framework, such disturbance is actively estimated using the ESO and canceled in the control law, in the absence of an accurate mathematical model of the plant.

In this chapter, for simplicity and easy understanding, a third order ADRC is presented for controlling a second order system. This chapter begins with the ESO

design, followed by the ADRC controller design. Section 3.3 shows the simulation and hardware tests to demonstrate the effectiveness of the ESO and the ADRC.

3.1 Extended State Observer

Consider a generally nonlinear time-varying second order dynamic system

$$\ddot{y}(t) = f(\dot{y}(t), y(t), w(t)) + bu(t). \tag{3.1}$$

where w is the external disturbance and b is a given constant. Here $f(\dot{y}(t), y(t), w(t))$, or simply denoted as f, represents the nonlinear time-varying dynamics of the plant that is unknown. That is, for this plant, only the order and the parameter b are given. The ADRC is a unique method designed to tackle this problem. It is centered around estimation of, and compensation for, f. To this end, assuming f is differentiable and let $h = \dot{f}$, (3.1) can be written in an augmented state space form

$$\begin{aligned} \dot{x}_1 &= x_2 \\ \dot{x}_2 &= x_3 + +bu \\ \dot{x}_3 &= h(x, u, w, \dot{w}) \\ y &= x_1 \end{aligned} \tag{3.2}$$

where $x = [x_1, x_2, x_3]^T$. An ESO of (3.2) will estimate the derivatives of y and f since (3.2) is now a state in the extended state model. With u and y as inputs, the ESO of (3.2) is given as

$$\begin{aligned} \dot{\hat{x}}_1 &= \hat{x}_2 + l_1(x_1 - \hat{x}_1) \\ \dot{\hat{x}}_2 &= \hat{x}_3 + l_2(x_1 - \hat{x}_1) + bu \\ \dot{\hat{x}}_3 &= l_3(x_1 - \hat{x}_1), \end{aligned} \tag{3.3}$$

where $\hat{x} = [\hat{x}_1, \hat{x}_2, \hat{x}_3]^T$, and $l_i, i = 1, 2, 3$, are the observer gain parameters to be chosen. The observer gains are chosen such that the characteristic polynomial $s^3 +$

$l_1 s^2 + l_2 s + l_3$ is Hurwitz. For tuning simplicity, all the observer poles are placed at $-\omega_o$. It results in the characteristic polynomial of (3.3) to be

$$\lambda_o(s) = s^3 + l_1 s^2 + l_2 s + l_3 = (s + \omega_o)^3 \tag{3.4}$$

where ω_o is the observer bandwidth and $L = \begin{bmatrix} 3\omega_o & 3\omega_o^2 & \omega_o^3 \end{bmatrix}^T$.

Generally, the larger the observer bandwidth is, the more accurate the estimation will be. However, a large observer bandwidth will increase noise sensitivity. Therefore a proper observer bandwidth should be selected in a compromise between the tracking performance and the noise tolerance.

3.2 Controller Design

Once the observer is designed and well tuned, its outputs will track x_1, x_2, and x_3 respectively. By canceling the effect of f using $\hat{x}_3$, the ADRC actively compensates for f in real time. The ADRC control law is given by

$$u = \frac{k_1 (r - \hat{x}_1) + k_2 (\dot{r} - \hat{x}_2) - \hat{x}_3 + \ddot{r}}{b} \tag{3.5}$$

where r is the reference signal, k_1 and k_2 are the controller gain parameters selected to make $s^2 + k_2 s + k_1$ Hurwitz. For simplicity, let $k_1 = \omega_c^2, k_2 = 2\omega_c$, where ω_c is the controller bandwidth. The closed-loop system becomes

$$\ddot{y} = (f - \hat{x}_3) + k_1 (r - \hat{x}_1) + k_2 (\dot{r} - \hat{x}_2) + \ddot{r}. \tag{3.6}$$

Note that with a well-designed ESO, the first term in the right hand side (RHS) of (3.6) is negligible and the rest of the terms in the RHS of (3.6) constitute a PD controller with a feedforward gain.

In practice, the controller bandwidth, ω_c, is tuned based on how fast and steady we want the output to track the set point. A large controller bandwidth generally

increases the response speed but it may push the system to its limit, leading to oscillations or even instability. Thus the controller bandwidth should be adjusted based on the competing requirements of performance and stability margin, together with noise sensitivity. In addition, a large controller bandwidth usually increases the magnitude and rate of change in control signal, and therefore the operation cost. The observer is tuned in a similar way: adjusting its bandwidth, ω_o, for a trade off between tracking performance and noise sensitivity.

The primary reason for this particular parameterization and tuning method is practicality: the observer and feedback gains must be easily tunable by most engineers, who are usually familiar with the concept and implications of bandwidth. It is advantageous that engineers could use a completely new design method without losing the critical insight gained from classical control: frequency response.

The effectiveness of the ESO and the ADRC is shown as below through simulation tests and hardware implementation.

3.3 Simulation and Hardware Tests

Two examples are given below for illustration purposes. One is a simulation study applying the ESO and the ADRC to a nonlinear plant to see how they perform with three different levels of knowledge on the plant dynamics. The other is a hardware test showing the effectiveness of ESO and ADRC in a real motion control environment. Section 3.3 has been presented in [76][1].

[1] ©[2007] IEEE.

3.3.1 A Simulation Case Study

Consider the following nonlinear system

$$\ddot{y} = \dot{y}^3 + y + w + u. \tag{3.7}$$

Rewrite (3.7) as

$$\ddot{y} = f + bu \tag{3.8}$$

where f represents the summation of the plant dynamics $\dot{y}^3 + y$ and the external disturbance w.

Note that for a second order plant, the ESO is of the third order, where $\hat{x}_3$ is an estimate of f. With a well-tuned observer, the control law

$$u = \frac{u_0 + \ddot{r} - \hat{x}_3}{b}, \tag{3.9}$$

should approximately reduces the original plant (3.8) to a double integral one, i.e.

$$\ddot{y} \approx u_0. \tag{3.10}$$

With the plant reduced to (3.10), a simple PD controller of the form

$$u_0 = k_p(r - \hat{x}_1) + k_d(\dot{r} - \hat{x}_2) \tag{3.11}$$

is usually sufficient to make the output track r, the desired trajectory, where $k_p = \omega_c^2, k_d = 2\omega_c$.

The ESO tracking performance is demonstrated in Figure 1 under three different scenarios: 1) f is completely unknown; 2) only partial internal dynamics information of the plant is given, i.e. $f_{\text{partial}} = \dot{y}^3$; 3) the internal dynamics of the plant f_{in} is completely known, i.e. $f_{\text{in}} = \dot{y}^3 + y$ is given. In this simulation, the tuning parameters are $\omega_c = 4.5$ rad/sec and $\omega_o = 20$ rad/sec. Figure 1 shows the observer errors for three cases using a step input at $t = 1$ second as the excitation and a pulse

disturbance with the amplitude of ±20, the period of 4 seconds, the pulse width 5% of the period, and the phase delay of 4 seconds. The ADRC performance with different ESOs is shown in Figure 2. From Figure 1 and Figure 2, it can be observed that the observer error decreases as the model information is incorporated into the ESO, and so does the tracking error of the control loop.

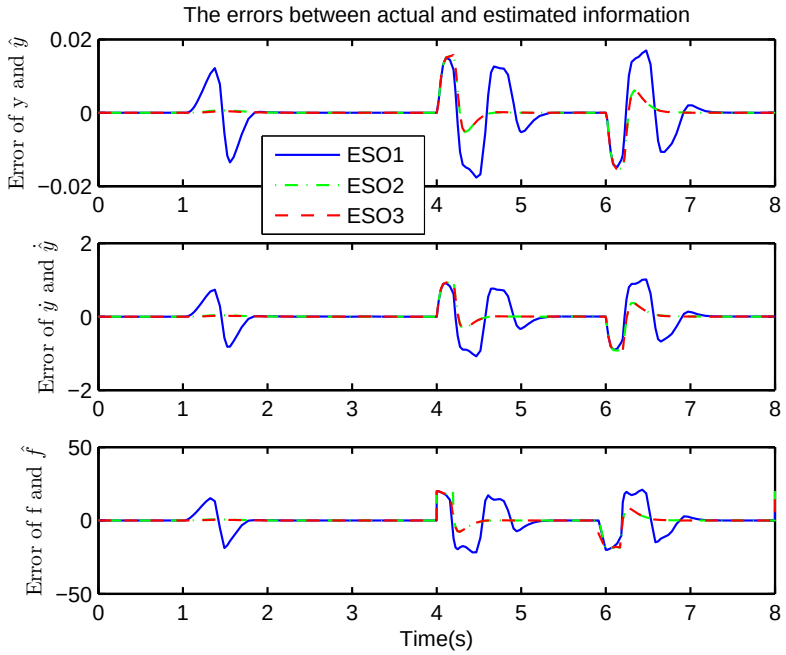

Figure 1: The errors between actual and estimated information. (ESO1: without plant information; ESO2: with partial plant information; ESO3: with complete plant information. Note that ESO2 and ESO3 are almost overlapped.)

3.3.2 A Motion Control Hardware Test

Motion control applications can be found in almost every sector of industry, from factory automation and robotics to high-tech computer hard-disk drives. They are used to regulate mechanical motions in terms of position, velocity, and acceleration, and/or to coordinate the motions of multiple axes or machine parts. In this case study, an industrial motion control test bed [77] is used to verify if the plant dynamics can indeed be estimated in real time, as shown in the mathematical analysis.

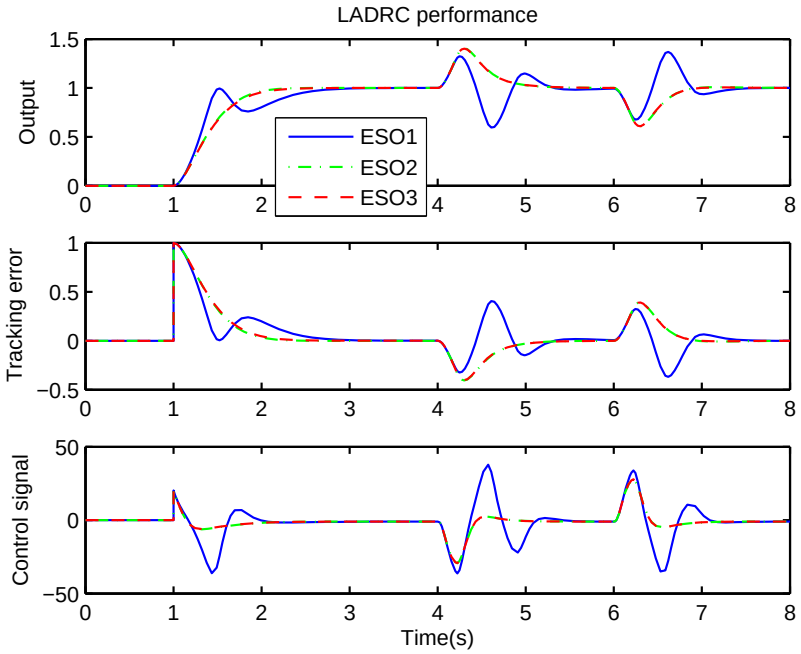

Figure 2: The ADRC performance with different ESOs for the nonlinear system. (ESO1: without plant information; ESO2: with partial plant information; ESO3: with complete plant information. Note that ESO2 and ESO3 are almost overlapped.)

The experimental setup includes a PC-based control platform and a DC brushless servo system, which is shown in Figure 3. The servo system includes two motors (one as an actuator and the other as the disturbance source), a power amplifier, and an encoder which provides the position measurement. The inertia, friction, and backlash are all adjustable, making it convenient to test the control algorithms. A Pentium 133 MHz PC running in DOS is programmed as the controller. It contains a data acquisition board for digital to analog conversion and a counter board to read the position encoder output in the servo system. The sampling frequency is 1 KHz. The output of the controller is limited to ± 3.5 V. The drive system has a dead zone of ± 0.5 V. The system is approximated as a second-order plant of the form

$$\ddot{y}(t) = f(y(t), \dot{y}(t), w(t)) + bu(t) \tag{3.12}$$

where $y(t)$ is the position output, b is a constant, $u(t)$ is the control voltage sent to the power amplifier that drives the motor, $w(t)$ is the external disturbance, and

$f\left(y\left(t\right),\dot{y}\left(t\right),w\left(t\right)\right)$ represents the combined effect of internal dynamics and external disturbances of the plant.

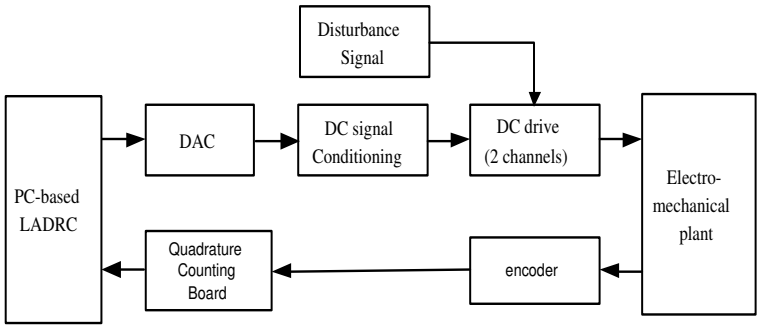

Figure 3: A diagram for DC brushless servo system.

How close (3.10) is to a double integral plant will be an indicator of how effective the observer is. Figure 4 shows the output comparison of an ideal double integrator, simulation test and hardware test of the original system (3.12) compensated by (3.9), where $\hat{x}_3$ is obtained from (4.13), with $b_0 = 25$ and $\omega_o = 300$ rad/sec. Note that b_0 is the approximate value of b in (3.12). The closeness of the three curves in Figure 4 confirms, beyond doubt, that the ESO is capable of extracting information from the input-output data on the unknown dynamics and disturbances. Moreover, this can be done in such a simple and effective manner that it makes the practical application straightforward.

The ADRC is tested in the Educational Control Products (ECP) motion control test bed with the tuning parameters selected as $\omega_c = 50$ rad/sec and $\omega_o = 100$ rad/sec, where the ESO is employed. As a comparison base, the hardware tests of the ADRC, for the nominal case and the case with the inertia increased by a factor of two and a 15% torque disturbance applied at $t = 2$ seconds, even though the controller parameters ω_c, ω_o and b_0 are kept unchanged, the ADRC demonstrates remarkable consistency in the presence of a significant disturbance and dynamic variation. The performance is shown in Figure 5. Such performance can only be attributed to the

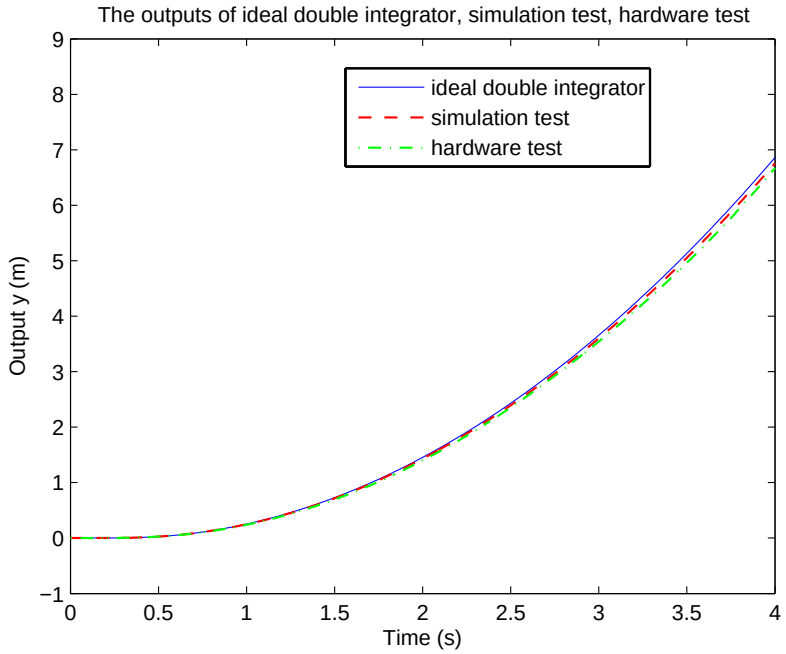

Figure 4: The output comparison among an ideal double integrator, simulation test, and hardware test.

ability of the ESO in obtaining an accurate estimation of the combined effect of plant dynamics and external disturbances in real time.

3.4 Summary

In this chapter, the ideas of the ESO design and the controller design of the ADRC are presented. The simulation and hardware tests shown in Section 3.3 verify the high disturbance rejection and robustness performance of the ESO and the ADRC.

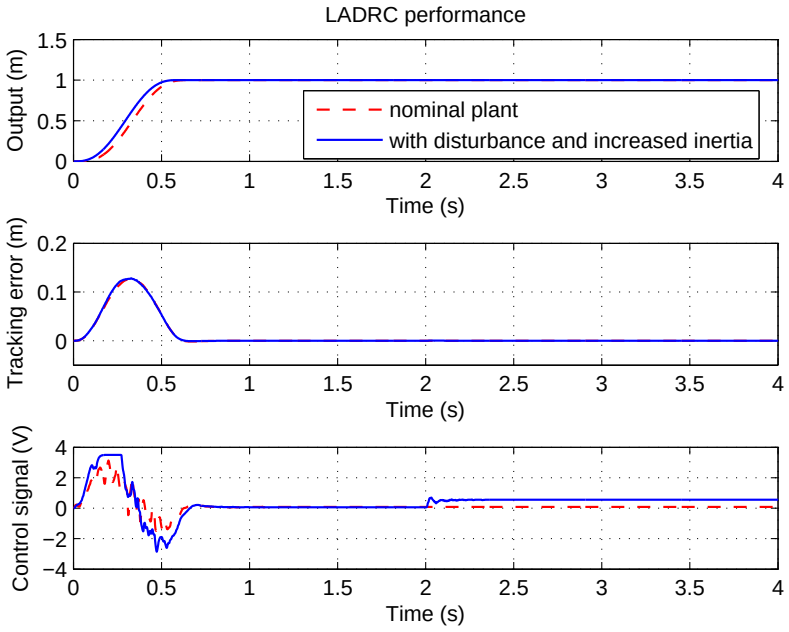

Figure 5: The performance for ECP Model 220 under the control of ADRC.

CHAPTER IV

STABILITY ANALYSIS

The ADRC has been extensively applied to nonlinear time-varying plants that are largely unknown. This chapter concerns with questions: 1) for a physical plant to be controlled, whether or not its internal dynamics and external disturbances can be realistically estimated in real time from its input-output data by the ESO; 2) whether or not there is an assurance for stability of the ADRC. In this chapter, it is shown that, for an n^{th} order plant, the answers to the above questions are indeed yes.

In particular, for the ESO, it is shown that the estimation error 1) converges to the origin asymptotically when the model of the plant is given; 2) is bounded and the error upper bound monotonously decreases with the bandwidth of the observer when the plant model is mostly unknown. For the ADRC, asymptotic stability is established where the plant dynamics is completely known. In the face of large dynamic uncertainties, the tracking error and its up to the $(n-1)^{st}$ derivatives are shown to be bounded. Furthermore, it is demonstrated that the closed-loop tracking error upper bounds, in general, monotonously decrease with the bandwidths of the controller and the observer.

Note that this is not another parameter estimation algorithm in the framework of adaptive control. It applies to a large class of nonlinear, time-varying processes with unknown dynamics.

This chapter is organized as follows. Section 4.1 analyzes the ESO convergence. Section 4.2 shows the ADRC stability. The chapter ends with a summary in Section 4.3. Note that Some contents of this chapter are extracted from [78][1].

First we want to establish the convergence of the ESO.

4.1 Analysis of ESO Error Dynamics

In this section, it is shown that: 1) with given plant dynamics, the dynamic system describing the estimation error is asymptotically stable; 2) with plant dynamics largely unknown, the ESO can estimate the unknown dynamics and disturbances and the estimation error upper bound of the ESO monotonously decreases with the observer bandwidth.

Consider a generally nonlinear time-varying dynamic system with single-input, u, and single-output, y,

$$y^{(n)}(t) = f(y^{(n-1)}(t), y^{(n-2)}(t), \cdots, y(t), w(t)) + bu(t). \tag{4.1}$$

where w is the external disturbance and b is a given constant. Here $f\left(y^{(n-1)}(t), y^{(n-2)}(t), \cdots, y(t), w(t)\right)$, or simply denoted as f, represents the nonlinear time-varying dynamics of the plant that is unknown. That is, for this plant, only the order and the parameter b are given. The ADRC is a unique method designed to tackle this problem. It is centered around estimation of, and compensation for, f. To this end, assuming f is differentiable and let $h = \dot{f}$, (4.1) can be written in an augmented

[1] ©[2007] IEEE.

state space form

$$\begin{aligned}
\dot{x}_1 &= x_2 \\
&\vdots \\
\dot{x}_{n-1} &= x_n \\
\dot{x}_n &= x_{n+1} + bu \\
\dot{x}_{n+1} &= h\left(x, u, w, \dot{w}\right) \\
y &= x_1
\end{aligned} \tag{4.2}$$

where $x = [x_1, x_2, \cdots, x_{n+1}]^T \in \mathbb{R}^{n+1}$, $u \in \mathbb{R}$ and $y \in \mathbb{R}$ are the state, input and output of the system, respectively. It is assumed that the order of the plant and the parameter b are given. Any state observer of (4.2), will estimate the derivatives of y and f since the latter is now a state in the extended state model. Such observers are known as the ESO. The convergence of the estimation error dynamics for the ESO is shown below.

4.1.1 Convergence of the ESO with the Given Model of the Plant

First the convergence of the ESO for a system with a given h is shown. With u and y as inputs and the function h given, the ESO of (4.2) is given as

$$\begin{aligned}
\dot{\hat{x}}_1 &= \hat{x}_2 + l_1\left(x_1 - \hat{x}_1\right) \\
&\vdots \\
\dot{\hat{x}}_{n-1} &= \hat{x}_n + l_{n-1}\left(x_1 - \hat{x}_1\right) \\
\dot{\hat{x}}_n &= \hat{x}_{n+1} + l_n\left(x_1 - \hat{x}_1\right) + bu \\
\dot{\hat{x}}_{n+1} &= l_{n+1}\left(x_1 - \hat{x}_1\right) + h\left(\hat{x}, u, w, \dot{w}\right)
\end{aligned} \tag{4.3}$$

where $\hat{x} = [\hat{x}_1, \hat{x}_2, \cdots, \hat{x}_{n+1}]^T \in \mathbb{R}^{n+1}$, and $l_i, i = 1, 2, \cdots, n+1$, are the observer gain parameters to be chosen. In particular, let us consider a special case where the gains

are chosen as

$$[l_1, l_2, \cdots, l_{n+1}] = \left[\omega_o\alpha_1, \omega_o^2\alpha_2, \cdots, \omega_o^{n+1}\alpha_{n+1}\right] \tag{4.4}$$

with $\omega_o > 0$. Here $\alpha_i, i = 1, 2, \cdots, n+1$, are selected such that the characteristic polynomial $s^{n+1} + \alpha_1 s^n + \cdots + \alpha_n s + \alpha_{n+1}$ is Hurwitz. For simplicity, let $s^{n+1} + \alpha_1 s^n + \cdots + \alpha_n s + \alpha_{n+1} = (s+1)^{n+1}$ where $\alpha_i = \frac{(n+1)!}{i!(n+1-i)!}$, $i = 1, 2, \cdots, n+1$. Then the characteristic polynomial of (4.3) is

$$\lambda_o(s) = s^{n+1} + \omega_o\alpha_1 s^n + \cdots + \omega_o^n\alpha_n s + \omega_o^{n+1}\alpha_{n+1} = (s+\omega_o)^n. \tag{4.5}$$

and ω_o, the observer bandwidth, becomes the only tuning parameter of the observer.

Let $\tilde{x}_i = x_i - \hat{x}_i, i = 1, 2, \cdots, n+1$. From (4.2) and (4.3), the observer estimation error can be shown as

$$\begin{aligned}
\dot{\tilde{x}}_1 &= \tilde{x}_2 - \omega_o\alpha_1\tilde{x}_1 \\
&\vdots \\
\dot{\tilde{x}}_{n-1} &= \tilde{x}_n - \omega_o^{n-1}\alpha_{n-1}\tilde{x}_1 \\
\dot{\tilde{x}}_n &= \tilde{x}_{n+1} - \omega_o^n\alpha_n\tilde{x}_1 \\
\dot{\tilde{x}}_{n+1} &= h(x, u, w, \dot{w}) - h(\hat{x}, u, w, \dot{w}) - \omega_o^{n+1}\alpha_{n+1}\tilde{x}_1.
\end{aligned} \tag{4.6}$$

Now let $\varepsilon_i = \frac{\tilde{x}_i}{\omega_o^{i-1}}, i = 1, 2, \cdots, n+1$, then (4.6) can be rewritten as

$$\dot{\varepsilon} = \omega_o A\varepsilon + B\frac{h(x, u, w, \dot{w}) - h(\hat{x}, u, w, \dot{w})}{\omega_o^n} \tag{4.7}$$

where $A = \begin{bmatrix} -\alpha_1 & 1 & 0 & \cdots & 0 \\ -\alpha_2 & 0 & 1 & \cdots & 0 \\ \vdots & \vdots & \ddots & \vdots & \vdots \\ -\alpha_n & 0 & \cdots & 0 & 1 \\ -\alpha_{n+1} & 0 & \cdots & 0 & 0 \end{bmatrix}$, $B = [0\ 0\ \cdots\ 0\ 1]^T$. Here A is Hurwitz for the $\alpha_i, i = 1, 2, \cdots, n+1$, chosen above.

Theorem 1. *Assuming $h(x,u,w,\dot{w})$ is globally Lipschitz with respect to x, there exists a constant $\omega_o > 0$, such that $\lim_{t\to\infty} \tilde{x}_i(t) = 0, i = 1,2,\cdots,n+1$.*

Proof. Since A is Hurwitz, there exists a unique positive definite matrix P such that $A^TP + PA = -I$. Choose the Lyapunov function as $V(\varepsilon) = \varepsilon^T P\varepsilon$. Hence $\dot{V}(\varepsilon) = \frac{\partial V(\varepsilon)}{\partial \varepsilon}\dot{\varepsilon}$, where

$$\frac{\partial V(\varepsilon)}{\partial \varepsilon} = \frac{\partial\left(\varepsilon^T P\varepsilon\right)}{\partial \varepsilon} = 2\varepsilon^T P, \tag{4.8}$$

and

$$\begin{aligned}
\dot{V}(\varepsilon) &= 2\varepsilon^T P\dot{\varepsilon} \\
&= 2\varepsilon^T P\left[\omega_o A\varepsilon + B\frac{h(x,u,w,\dot{w}) - h(\hat{x},u,w,\dot{w})}{\omega_o^n}\right] \\
&= \omega_o\varepsilon^T PA\varepsilon + \omega_o\varepsilon^T A^T P\varepsilon + 2\varepsilon^T PB\frac{h(x,u,w,\dot{w}) - h(\hat{x},u,w,\dot{w})}{\omega_o^n} \\
&= -\omega_o\|\varepsilon\|^2 + 2\varepsilon^T PB\frac{h(x,u,w,\dot{w}) - h(\hat{x},u,w,\dot{w})}{\omega_o^n}.
\end{aligned} \tag{4.9}$$

Since the function $h(x,u,w,\dot{w})$ is globally Lipschitz with respect to x, that is, there exists a constant c' such that $|h(x,u,w,\dot{w}) - h(\hat{x},u,w,\dot{w})| \le c'\|x-\hat{x}\|$ for all $x, \hat{x}, u, w$, and $\dot{w}$, it follows that

$$2\varepsilon^T PB\frac{|h(x,u,w,\dot{w}) - h(\hat{x},u,w,\dot{w})|}{\omega_o^n} \le 2\varepsilon^T PBc'\frac{\|x-\hat{x}\|}{\omega_o^n}. \tag{4.10}$$

When $\omega_o \ge 1$, one has $\frac{\|x-\hat{x}\|}{\omega_o^n} = \frac{\|\tilde{x}\|}{\omega_o^n} = \frac{\left\|\sqrt{\varepsilon_1^2+\varepsilon_2^2\omega_o^2+\varepsilon_3^2\omega_o^4+\cdots+\varepsilon_{n+1}^2\omega_o^{2n}}\right\|}{\omega_o^n} \le \|\varepsilon\|$. Therefore, we obtain

$$\begin{aligned}
2\varepsilon^T PB\frac{|h(x,u,w,\dot{w}) - h(\hat{x},u,w,\dot{w})|}{\omega_o^n} &\le 2\varepsilon^T PBc'\frac{\|x-\hat{x}\|}{\omega_o^n} \\
&\le 2\varepsilon^T PBc'\|\varepsilon\| \\
&\le \|\varepsilon\|^2 + \|PBc'\|^2\|\varepsilon\|^2 \\
&= c\|\varepsilon\|^2
\end{aligned} \tag{4.11}$$

where $c = 1 + \|PBc'\|^2$. From (4.9) and (4.11), one has

$$\dot{V}(\varepsilon) \leq -(\omega_o - c)\|\varepsilon\|^2. \tag{4.12}$$

That is, $\dot{V}(\varepsilon) < 0$ if $\omega_o > c$. Therefore, $\lim_{t\to\infty} \tilde{x}_i(t) = 0, i = 1, 2, \cdots, n+1$, for $\omega_o > c$. Q.E.D.

In summary, it is proven that, when the plant model is given, the dynamic system describing the estimation error of the ESO (4.3) is asymptotically stable.

4.1.2 Convergence of the ESO with Plant Dynamics Largely Unknown

In this section, we consider that the plant dynamics represented by f is mostly unknown. In this case, the ESO in (4.3) now takes the form of

$$\begin{aligned}
\dot{\hat{x}}_1 &= \hat{x}_2 + l_1(x_1 - \hat{x}_1) \\
&\vdots \\
\dot{\hat{x}}_{n-1} &= \hat{x}_n + l_{n-1}(x_1 - \hat{x}_1) \\
\dot{\hat{x}}_n &= \hat{x}_{n+1} + l_n(x_1 - \hat{x}_1) + bu \\
\dot{\hat{x}}_{n+1} &= l_{n+1}(x_1 - \hat{x}_1).
\end{aligned} \tag{4.13}$$

Consequently, the observer estimation error in (4.6) becomes

$$\begin{aligned}
\dot{\tilde{x}}_1 &= \tilde{x}_2 - \omega_o \alpha_1 \tilde{x}_1 \\
&\vdots \\
\dot{\tilde{x}}_{n-1} &= \tilde{x}_n - \omega_o^{n-1} \alpha_{n-1} \tilde{x}_1 \\
\dot{\tilde{x}}_n &= \tilde{x}_{n+1} - \omega_o^n \alpha_n \tilde{x}_1 \\
\dot{\tilde{x}}_{n+1} &= h(x, u, w, \dot{w}) - \omega_o^{n+1} \alpha_{n+1} \tilde{x}_1
\end{aligned} \tag{4.14}$$

and Equation (4.7) is now

$$\dot{\varepsilon} = \omega_o A\varepsilon + B\frac{h(x, u, w, \dot{w})}{\omega_o^n}. \tag{4.15}$$

Theorem 2. *Assuming $h(x,u,w,\dot{w})$ is bounded, there exist a constant $\sigma_i > 0$ and a finite $T_1 > 0$ such that $|\tilde{x}_i(t)| \leq \sigma_i, i = 1,2,\cdots,n+1, \forall t \geq T_1 > 0$ and $\omega_o > 0$. Furthermore, $\sigma_i = \mathrm{O}\left(\frac{1}{\omega_o^k}\right)$, for some positive integer k.*

Proof. Solving (4.15), it follows that

$$\varepsilon(t) = e^{\omega_o A t}\varepsilon(0) + \int_0^t e^{\omega_o A(t-\tau)} B \frac{h(x(\tau),u,w,\dot{w})}{\omega_o^n} d\tau. \tag{4.16}$$

Let

$$p(t) = \int_0^t e^{\omega_o A(t-\tau)} B \frac{h(x(\tau),u,w,\dot{w})}{\omega_o^n} d\tau, \tag{4.17}$$

since $h(x(\tau),u,w,\dot{w})$ is bounded, that is, $|h(x(\tau),u,w,\dot{w})| \leq \delta$, where δ is a positive constant, for $i = 1,2,\cdots,n+1$, we have

$$\begin{aligned}
|p_i(t)| &\leq \frac{\int_0^t \left[e^{\omega_o A(t-\tau)}B\right]_i |h(x(\tau),u,w,\dot{w})|\, d\tau}{\omega_o^n} \\
&\leq \frac{\delta \int_0^t \left[e^{\omega_o A(t-\tau)}B\right]_i d\tau}{\omega_o^n} \\
&= \frac{\delta}{\omega_o^n}\left\{\left[-(\omega_o A)^{-1} e^{\omega_o A(t-\tau)}\Big|_0^t\right] B\right\}_i \\
&\leq \frac{\delta}{\omega_o^{n+1}}\left[\left|\left(A^{-1}B\right)_i\right| + \left|\left(A^{-1}e^{\omega_o A t}B\right)_i\right|\right].
\end{aligned} \tag{4.18}$$

For A and B defined in (4.7), $A^{-1} = \begin{bmatrix} 0 & 0 & 0 & \cdots & -\frac{1}{\alpha_{n+1}} \\ 1 & 0 & 0 & \cdots & -\frac{\alpha_1}{\alpha_{n+1}} \\ 0 & 1 & 0 & \cdots & -\frac{\alpha_2}{\alpha_{n+1}} \\ \vdots & \vdots & \vdots & \ddots & \vdots \\ 0 & 0 & \cdots & 1 & -\frac{\alpha_n}{\alpha_{n+1}} \end{bmatrix}$,

and

$$\begin{aligned}\left|\left(A^{-1}B\right)_i\right| &= \left|\begin{bmatrix} -\frac{1}{\alpha_{n+1}} \\ -\frac{\alpha_1}{\alpha_{n+1}} \\ \vdots \\ -\frac{\alpha_n}{\alpha_{n+1}} \end{bmatrix}_i\right| \\ &= \begin{cases} \left.\frac{1}{\alpha_{n+1}}\right|_{i=1} \\ \left.\frac{\alpha_{i-1}}{\alpha_{n+1}}\right|_{i=2,\cdots,\, n+1} \end{cases} \\ &\leq \nu \end{aligned} \tag{4.19}$$

where $\nu = \max\limits_{i=2,\cdots,n+1}\left\{\frac{1}{\alpha_{n+1}}, \frac{\alpha_{i-1}}{\alpha_{n+1}}\right\}$. Since A is Hurwitz, there exists a finite time $T_1 > 0$ such that

$$\left|\left[e^{\omega_o A t}\right]_{ij}\right| \leq \frac{1}{\omega_o^{n+1}} \tag{4.20}$$

for all $t \geq T_1, i, j = 1, 2, \cdots, n+1$. Hence

$$\left|\left[e^{\omega_o A t} B\right]_i\right| \leq \frac{1}{\omega_o^{n+1}} \tag{4.21}$$

for all $t \geq T_1, i = 1, 2, \cdots, n+1$. Note that T_1 depends on $\omega_o A$. Let $A^{-1} = \begin{bmatrix} s_{11} & \cdots & s_{1,n+1} \\ \vdots & \ddots & \vdots \\ s_{n+1,1} & \cdots & s_{n+1,n+1} \end{bmatrix}$ and $e^{\omega_o A t} = \begin{bmatrix} d_{11} & \cdots & d_{1,n+1} \\ \vdots & \ddots & \vdots \\ d_{n+1,1} & \cdots & d_{n+1,n+1} \end{bmatrix}$. One has

$$\begin{aligned}\left|\left(A^{-1}e^{\omega_o A t}B\right)_i\right| &= \left|s_{i,1}d_{1,n+1} + s_{i,2}d_{2,n+1} + \cdots + s_{i,n+1}d_{n+1,n+1}\right| \\ &\leq \frac{|s_{i,1}| + |s_{i,2}| + \cdots + |s_{i,n+1}|}{\omega_o^{n+1}} \\ &= \begin{cases} \left.\frac{1}{\omega_o^{n+1}\alpha_{n+1}}\right|_{i=1} \\ \left.\frac{1}{\omega_o^{n+1}}\left(1 + \frac{\alpha_{i-1}}{\alpha_{n+1}}\right)\right|_{i=2,\cdots,n+1} \end{cases} \\ &\leq \frac{\mu}{\omega_o^{n+1}} \end{aligned} \tag{4.22}$$

for all $t \geq T_1,\ i = 1, 2, \cdots, n+1$, where $\mu = \max\limits_{i=2,\cdots,n+1} \left\{ \frac{1}{\alpha_{n+1}},\ 1 + \frac{\alpha_{i-1}}{\alpha_{n+1}} \right\}$. From (4.18), (4.19), and (4.22), we obtain

$$|p_i(t)| \leq \frac{\delta\nu}{\omega_o^{n+1}} + \frac{\delta\mu}{\omega_o^{2n+2}} \tag{4.23}$$

for all $t \geq T_1, i = 1, 2, \cdots, n+1$. Let $\varepsilon_{sum}(0) = |\varepsilon_1(0)| + |\varepsilon_2(0)| + \cdots + |\varepsilon_{n+1}(0)|$. It follows that

$$\begin{aligned} \left| \left[e^{\omega_o A t} \varepsilon(0) \right]_i \right| &= |d_{i,1}\varepsilon_1(0) + d_{i,2}\varepsilon_2(0) + \cdots + d_{i,n+1}\varepsilon_{n+1}(0)| \\ &\leq \frac{\varepsilon_{sum}(0)}{\omega_o^{n+1}} \end{aligned} \tag{4.24}$$

for all $t \geq T_1, i = 1, 2, \cdots, n+1$. From (4.16), one has

$$|\varepsilon_i(t)| \leq \left| \left[e^{\omega_o A t} \varepsilon(0) \right]_i \right| + |p_i(t)|. \tag{4.25}$$

Let $\tilde{x}_{sum}(0) = |\tilde{x}_1(0)| + |\tilde{x}_2(0)| + \cdots + |\tilde{x}_{n+1}(0)|$. According to $\varepsilon_i = \frac{\tilde{x}_i}{\omega_o^{i-1}}$ and Equations (4.23)-(4.25), we have

$$\begin{aligned} |\tilde{x}_i(t)| &\leq \left| \frac{\varepsilon_{sum}(0)}{\omega_o^{n+1}} \right| \omega_o^{i-1} + |p_i(t)| \omega_o^{i-1} \\ &\leq \left| \frac{\tilde{x}_{sum}(0)}{\omega_o^{n+1}} \right| + \frac{\delta\nu}{\omega_o^{n-i+2}} + \frac{\delta\mu}{\omega_o^{2n-i+3}} \\ &= \sigma_i \end{aligned} \tag{4.26}$$

for all $t \geq T_1, i = 1, 2, \cdots, n+1$. Q.E.D.

In summary, it is proven that, in the absence of such model, the estimation error of the ESO (4.13) is bounded and its upper bound monotonously decreases with the observer bandwidth, as shown in (4.26).

The stability characteristics of the ADRC, where the ESO is employed, is analyzed next.

4.2 Stability Characteristics of ADRC

In this section, it is shown that 1) with the given model of the plant, the closed-loop system is asymptotically stable; and 2) with plant dynamics largely unknown, the tracking error and its up to $(n-1)^{th}$ order derivatives of the ADRC are bounded and their upper bounds monotonously decrease with the observer and controller bandwidths.

Assume that the control design objective is to make the output of the plant in (1) follow a given, bounded, reference signal r, whose derivatives, $\dot{r}, \ddot{r}, \cdots, r^{(n)}$, are also bounded. Let $[r_1, r_2, \cdots, r_n, r_{n+1}]^T = [r, \dot{r}_1, \cdots, \dot{r}_{n-1}, \dot{r}_n]^T$. Employing the ESO of (4.2) in the form of (4.3) or (4.13), the ADRC control law is given as

$$u = \left[k_1 (r_1 - \hat{x}_1) + k_2 (r_2 - \hat{x}_2) + \cdots + k_n (r_n - \hat{x}_n) - \hat{x}_{n+1} + r_{n+1}\right] / b \tag{4.27}$$

where $k_i, i = 1, 2, \cdots, n$, are the controller gain parameters selected to make $s^n + k_n s^{n-1} + \cdots + k_1$ Hurwitz. The system (4.1) becomes

$$y^{(n)}(t) = \ (f - \hat{x}_{n+1}) + k_1 (r_1 - \hat{x}_1) + k_2 (r_2 - \hat{x}_2) + \cdots + k_n (r_n - \hat{x}_n) + r_{n+1}. \tag{4.28}$$

Note that with a well-designed ESO, the first term in the right hand side (RHS) of (4.28) is negligible and the rest of the terms in the RHS of (4.28) constitutes a generalized PD controller with a feedforward term. It generally works very well in applications but the issues to be addressed are: 1) the stability of the closed-loop system (4.28) and (4.3); and 2) the bound of the tracking error.

4.2.1 Convergence of the ADRC with the Given Model of the Plant

Consider

$$\dot{\eta}(t) = N\eta(t) + g(t), \tag{4.29}$$

where $\eta(t) = [\eta_1(t), \eta_2(t), \cdots, \eta_n(t)]^T \in \mathbb{R}^n$, $g(t) = [g_1(t), g_2(t), \cdots, g_n(t)]^T \in \mathbb{R}^n$, and N is an $n \times n$ matrix.

Lemma 1. *If N is Hurwitz and $\lim_{t\to\infty} \|g(t)\| = 0$, then $\lim_{t\to\infty} \|\eta(t)\| = 0$.*

Proof. In (4.29), since $\lim_{t\to\infty} \|g(t)\| = 0$, then for any $\phi > 0$, there is a finite time $T_2 > 0$ such that $\|g(t)\| \le \phi$ for all $t \ge T_2$. The response of (4.29) can be written as

$$\eta(t) = e^{Nt}\eta(0) + \int_0^t e^{N(t-\tau)} g(\tau)\, d\tau. \tag{4.30}$$

When $t \ge T_2$, we have

$$\begin{aligned} \|\eta(t)\| &= \left\| e^{Nt}\eta(0) + \int_0^{T_2} e^{N(t-\tau)} g(\tau)\, d\tau + \int_{T_2}^t e^{N(t-\tau)} g(\tau)\, d\tau \right\| \\ &\le \left\| e^{Nt}\eta(0) \right\| + \left\| e^{Nt} \right\| \left\| \int_0^{T_2} e^{-N\tau} g(\tau)\, d\tau \right\| + \int_{T_2}^t \left\| e^{N(t-\tau)} \right\| \phi d\tau. \end{aligned} \tag{4.31}$$

Now consider the third term of right hand side of (4.31). For N, there is nonsingular matrix J and block diagonal matrix $\Lambda = block\, diag\{\Lambda_1, \cdots, \Lambda_m\}$ such that

$$N = J\Lambda J^{-1} \tag{4.32}$$

and each Λ_i has a single eigenvalue λ_i with its algebraic multiplicities being q_i. Suppose $\lambda_1 \ge \lambda_2 \ge \cdots \ge \lambda_m$. Let $q = \max\{q_1, q_2, \cdots, q_m\}$. Let us choose $\|\cdot\|_1$ or $\|\cdot\|_\infty$ for the matrix norm. It follows that [79]

$$\left\| e^{\Lambda(t-\tau)} \right\| \le e^{\lambda_1(t-\tau)} \sum_{k=0}^{q-1} c_k (t-\tau)^k, \quad \forall t \ge \tau, \tag{4.33}$$

where c_k are positive constants. Note that

$$\begin{aligned} \left\| e^{N(t-\tau)} \right\| &= \left\| J e^{\Lambda(t-\tau)} J^{-1} \right\| \\ &\le \|J\| \left\| e^{\Lambda(t-\tau)} \right\| \left\| J^{-1} \right\|. \end{aligned} \tag{4.34}$$

Hence we have

$$\begin{aligned}
\|\eta(t)\| &\leq \left\|e^{Nt}\eta(0)\right\| + \left\|e^{Nt}\right\| \left\| \int_0^{T_2} e^{-N\tau} g(\tau)\, d\tau \right\| + \phi \|J\| \left\|J^{-1}\right\| \int_{T_2}^{t} \left\|e^{\Lambda(t-\tau)}\right\| d\tau \\
&\leq \left\|e^{Nt}\eta(0)\right\| + \left\|e^{Nt}\right\| \left\| \int_0^{T_2} e^{-N\tau} g(\tau)\, d\tau \right\| \\
&\quad + \phi \|J\| \left\|J^{-1}\right\| \sum_{k=0}^{q-1} c_k \int_{T_2}^{t} e^{\lambda_1(t-\tau)} (t-\tau)^k\, d\tau \\
&= \left\|e^{Nt}\eta(0)\right\| + \left\|e^{Nt}\right\| \left\| \int_0^{T_2} e^{-N\tau} g(\tau)\, d\tau \right\| + \phi \|J\| \left\|J^{-1}\right\| \cdot \\
&\quad \sum_{k=0}^{q-1} c_k \left\{ \frac{e^{\lambda_1(t-T_2)}}{\lambda_1^{k+1}} \sum_{j=0}^{k} (-1)^j \frac{k!}{(k-j)!} \left[\lambda_1 (t-T_2)\right]^{k-j} - \frac{(-1)^k k!}{\lambda_1^{k+1}} \right\} \\
&= \left\|e^{Nt}\eta(0)\right\| + \left\|e^{Nt}\right\| \left\| \int_0^{T_2} e^{-N\tau} g(\tau)\, d\tau \right\| \\
&\quad + e^{\lambda_1(t-T_2)} \phi \|J\| \left\|J^{-1}\right\| \sum_{k=0}^{q-1} c_k \frac{1}{\lambda_1^{k+1}} \sum_{j=0}^{k} (-1)^j \frac{k!}{(k-j)!} \left[\lambda_1 (t-T_2)\right]^{k-j} \\
&\quad + \phi \|J\| \left\|J^{-1}\right\| \sum_{k=0}^{q-1} c_k \frac{(-1)^k k!}{\lambda_1^{k+1}}. \qquad (4.35)
\end{aligned}$$

From (4.35), it can be seen that

$$\begin{aligned}
&\lim_{t\to\infty} \left\|e^{Nt}\eta(0)\right\| = 0 \\
&\lim_{t\to\infty} \left\|e^{Nt}\right\| \left\| \int_0^{T_2} e^{-N\tau} g(\tau)\, d\tau \right\| = 0 \qquad (4.36) \\
&\lim_{t\to\infty} \left\{ e^{\lambda_1(t-T_2)} \phi \|J\| \left\|J^{-1}\right\| \sum_{k=0}^{q-1} c_k \tfrac{1}{\lambda_1^{k+1}} \sum_{j=0}^{k} (-1)^j \tfrac{k!}{(k-j)!} \left[\lambda_1 (t-T_2)\right]^{k-j} \right\} = 0.
\end{aligned}$$

Therefore there exists $T_3 > T_2$ such that

$$\begin{aligned}
&\left\|e^{Nt}\eta(0)\right\| \leq \phi,\ \forall t \geqslant T_3, \\
&\left\|e^{Nt}\right\| \left\| \int_0^{T_2} e^{-N\tau} g(\tau)\, d\tau \right\| \leq \phi,\ \forall t \geq T_3, \qquad (4.37) \\
&e^{\lambda_1(t-T_2)} \phi \|J\| \left\|J^{-1}\right\| \left\{ \sum_{k=0}^{q-1} c_k \tfrac{1}{\lambda_1^{k+1}} \sum_{j=0}^{k} (-1)^j \tfrac{k!}{(k-j)!} \left[\lambda_1 (t-T_2)\right]^{k-j} \right\} \leq \phi,\ \forall t \geq T_3.
\end{aligned}$$

Let $c'' = \|J\| \|J^{-1}\| \sum_{k=0}^{q-1} c_k \frac{(-1)^k k!}{\lambda_1^{k+1}}$. Then we have

$$\|\eta(t)\| \leq (c''+3)\,\phi,\ \forall t \geq T_3. \tag{4.38}$$

Since ϕ can be arbitrarily small, it can be concluded that $\lim_{t\to\infty} \|\eta(t)\| = 0$.

Theorem 3. *Assuming $h(x,u,w,\dot{w})$ is globally Lipschitz with respect to x, there exist constants $\omega_o > 0$ and $\omega_c > 0$, such that the closed-loop system (4.28) and (4.3) is asymptotically stable.*

Proof. Define $e_i = r_i - x_i, i = 1, 2, \cdots, n$. From (4.27), one has

$$\begin{aligned} u &= [k_1(r_1 - \hat{x}_1) + \cdots + k_n(r_n - \hat{x}_n) - \hat{x}_{n+1} + r_{n+1}]/b \\ &= \{k_1[r_1 - (x_1 - \tilde{x}_1)] + \cdots + k_n[r_n - (x_n - \tilde{x}_n)] - (x_{n+1} - \tilde{x}_{n+1}) + r_{n+1}\}/b \\ &= [k_1(e_1 + \tilde{x}_1) + \cdots + k_n(e_n + \tilde{x}_n) - (x_{n+1} - \tilde{x}_{n+1}) + r_{n+1}\}/b. \end{aligned} \tag{4.39}$$

It follows that

$$\begin{aligned} \dot{e}_1 &= \dot{r}_1 - \dot{x}_1 = r_2 - x_2 = e_2, \\ &\vdots \\ \dot{e}_{n-1} &= \dot{r}_{n-1} - \dot{x}_{n-1} = r_n - x_n = e_n, \\ \dot{e}_n &= \dot{r}_n - \dot{x}_n = r_{n+1} - (x_{n+1} + bu) \\ &= r_{n+1} - x_{n+1} - [k_1(e_1 + \tilde{x}_1) + \cdots + k_n(e_n + \tilde{x}_n) - (x_{n+1} - \tilde{x}_{n+1}) + r_{n+1}] \\ &= -k_1(e_1 + \tilde{x}_1) - \cdots - k_n(e_n + \tilde{x}_n) - \tilde{x}_{n+1}. \end{aligned} \tag{4.40}$$

Let $e = [e_1, e_2, \cdots, e_n]^T \in \mathbb{R}^n, \tilde{x} = [\tilde{x}_1, \tilde{x}_2, \cdots, \tilde{x}_{n+1}]^T \in \mathbb{R}^{n+1}$, then

$$\dot{e}(t) = A_e e(t) + A_{\tilde{x}} \tilde{x}(t) \tag{4.41}$$

where $A_e = \begin{bmatrix} 0 & 1 & 0 & \cdots & 0 \\ 0 & 0 & 1 & \cdots & 0 \\ \vdots & \vdots & \ddots & \vdots & \vdots \\ 0 & 0 & \cdots & 0 & 1 \\ -k_1 & -k_2 & \cdots & -k_{n-1} & -k_n \end{bmatrix}$ and $A_{\tilde{x}} = \begin{bmatrix} 0 & 0 & 0 & \cdots & 0 \\ 0 & 0 & 0 & \cdots & 0 \\ \vdots & \vdots & \ddots & \vdots & \vdots \\ 0 & 0 & \cdots & 0 & 0 \\ -k_1 & -k_2 & \cdots & -k_n & -1 \end{bmatrix}$.

Since $k_i, i = 1, 2, \cdots, n$, are selected such that the characteristic polynomial $s^n + k_n s^{n-1} + \cdots + k_1$ is Hurwitz, A_e is Hurwitz. For tuning simplicity, we just let $s^n + k_n s^{n-1} + \cdots + k_1 = (s + \omega_c)^n$ where $\omega_c > 0$ and $k_i = \frac{n!}{(i-1)!(n+1-i)!}\omega_c^{n+1-i}$, $i = 1, 2, \cdots, n$. This makes ω_c, which is the controller bandwidth, the only tuning parameter to be adjusted for the controller.

From Theorem 1, $\lim\limits_{t\to\infty} \|A_{\tilde{x}}\tilde{x}(t)\| = 0$ if $h(x, u, w, \dot{w})$ is globally Lipschitz with respect to x. Since A_e is Hurwitz, according to Theorem 1 and Lemma 1, it can be concluded that: assuming $h(x, u, w, \dot{w})$ is globally Lipschitz with respect to x, there exist constants $\omega_o > 0$ and $\omega_c > 0$, such that $\lim\limits_{t\to\infty} e_i(t) = 0, i = 1, 2, \cdots, n$. Q.E.D.

From the above, it is shown that, with the given model of the plant, the closed-loop system (4.28) and (4.3) is asymptotically stable.

4.2.2 Convergence of the ADRC with Plant Dynamics Largely Unknown

Now we consider the case where the plant dynamics is largely unknown and the ESO in the form of (4.13) is used instead.

Theorem 4. *Assuming $h(x, u, w, \dot{w})$ is bounded, there exist a constant $\rho_i > 0$ and a finite time $T_5 > 0$ such that $|e_i(t)| \leq \rho_i, i = 1, 2, \cdots, n, \forall t \geq T_5 > 0$, $\omega_o > 0$, and $\omega_c > 0$. Furthermore, $\rho_i = \mathrm{O}\left(\frac{1}{\omega_c^j}\right)$ for some positive integer j.*

Proof. Solving (4.41), we have

$$e(t) = e^{A_e t}e(0) + \int_0^t e^{A_e(t-\tau)}A_{\tilde{x}}\tilde{x}(\tau)\,d\tau. \tag{4.42}$$

According to (4.41) and Theorem 2, one has

$$\begin{aligned} &[A_{\tilde{x}}\tilde{x}(\tau)]_{i=1,\cdots,n-1} = 0 \\ &|[A_{\tilde{x}}\tilde{x}(\tau)]_n| = |-k_1\tilde{x}_1(\tau) - \cdots - k_n\tilde{x}_n(\tau) - \tilde{x}_{n+1}(\tau)| \\ &\qquad\qquad \leqslant k_{sum}\sigma_i = \gamma, \forall t \geqslant T_1 \end{aligned} \tag{4.43}$$

where $k_{sum} = 1 + \sum_{i=1}^{n} k_i$. Similar to Theorem 3, choose $k_i = \frac{n!}{(i-1)!(n+1-i)!}\omega_c^{n+1-i}$, $i = 1, 2, \cdots, n$, such that A_e is Hurwitz. Define $\Psi = [0\ 0\ \cdots\ 0\ \gamma]^T$. Let $\varphi(t) = \int_0^t e^{A_e(t-\tau)} A_{\tilde{x}} \tilde{x}(\tau)\, d\tau$. It follows that

$$\begin{aligned} |\varphi_i(t)| &= \int_0^t \left[e^{A_e(t-\tau)} A_{\tilde{x}} \tilde{x}(\tau)\right]_i d\tau \\ &\leq \int_0^t \left[e^{A_e(t-\tau)}\Psi\right]_i d\tau \\ &= \left\{\left[-A_e^{-1}\, e^{A_e(t-\tau)}\Big|_0^t\right]\Psi\right\}_i \\ &\leq \left|\left(A_e^{-1}\Psi\right)_i\right| + \left|\left(A_e^{-1}e^{A_e t}\Psi\right)_i\right|. \end{aligned} \tag{4.44}$$

For A_e defined in (4.41), $A_e^{-1} = \begin{bmatrix} -\frac{k_2}{k_1} & -\frac{k_3}{k_1} & \cdots & -\frac{k_n}{k_1} & -\frac{1}{k_1} \\ 1 & 0 & \cdots & 0 & 0 \\ 0 & 1 & \cdots & 0 & 0 \\ \vdots & \vdots & \ddots & \vdots & \vdots \\ 0 & 0 & \cdots & 1 & 0 \end{bmatrix}$, and

$$\begin{aligned} \left|\left(A_e^{-1}\Psi\right)_1\right| &= \tfrac{\gamma}{k_1} = \tfrac{\gamma}{\omega_c^n} \\ \left|\left(A_e^{-1}\Psi\right)_i\right|_{i=2,\cdots,n} &= 0 \end{aligned} \tag{4.45}$$

Since A_e is Hurwitz, there exists a finite time $T_4 > 0$ such that

$$\left|\left[e^{A_e t}\right]_{ij}\right| \leqslant \frac{1}{\omega_c^{n+1}} \tag{4.46}$$

for all $t \geqslant T_4$, $i, j = 1, 2, \cdots, n$. Note that T_4 depends on A_e. Let $T_5 = \max\{T_1, T_4\}$. It follows that

$$\left|\left(e^{A_e t}\Psi\right)_i\right| \leqslant \frac{\gamma}{\omega_c^{n+1}} \tag{4.47}$$

for all $t \geqslant T_5$, $i = 1, 2, \cdots, n$, and

$$\left|\left(A_e^{-1}e^{A_e t}\Psi\right)_i\right| \leqslant \begin{cases} \left.\dfrac{1 + \sum_{i=2}^{n} k_i}{\omega_c^n}\dfrac{\gamma}{\omega_c^{n+1}}\right|_{i=1} \\ \left.\dfrac{\gamma}{\omega_c^{n+1}}\right|_{i=2,\cdots,n} \end{cases} \tag{4.48}$$

for all $t \geqslant T_5$. From (4.44), (4.45), and (4.48), we obtain

$$\begin{aligned} |\varphi_i(t)| &\leq \left|\left(A_e^{-1}\Psi\right)_i\right| + \left|\left(A_e^{-1}e^{A_e t}\Psi\right)_i\right| \\ &\leq \begin{cases} \left.\dfrac{\gamma}{\omega_c^n} + \dfrac{1+\sum_{i=2}^{n} k_i}{\omega_c^n}\dfrac{\gamma}{\omega_c^{n+1}}\right|_{i=1} \\ \left.\dfrac{\gamma}{\omega_c^{n+1}}\right|_{i=2,\cdots,n} \end{cases} \end{aligned} \tag{4.49}$$

for all $t \geqslant T_5$. Let $e^{A_e t} = \begin{bmatrix} o_{11} & \cdots & o_{1n} \\ \vdots & \ddots & \vdots \\ o_{n1} & \cdots & o_{nn} \end{bmatrix}$ and $e_{sum}(0) = |e_1(0)| + |e_2(0)| + \cdots + |e_n(0)|$. It follows that

$$\begin{aligned} \left|\left[e^{A_e t}e(0)\right]_i\right| &= |o_{i1}e_1(0) + o_{i2}e_2(0) + \cdots + o_{in}e_n(0)| \\ &\leq \frac{e_{sum}(0)}{\omega_c^{n+1}} \end{aligned} \tag{4.50}$$

for all $t \geq T_5,\ i = 1, 2, \cdots, n$. From (4.42), one has

$$|e_i(t)| \leqslant \left|\left[e^{A_e t}e(0)\right]_i\right| + |\varphi_i(t)|. \tag{4.51}$$

According to (4.43), (4.49)-(4.51), we have

$$\begin{aligned} |e_i(t)| &\leq \begin{cases} \left.\dfrac{e_{sum}(0)}{\omega_c^{n+1}} + \dfrac{k_{sum}\sigma_i}{\omega_c^n} + \dfrac{\left(1+\sum_{i=2}^{n} k_i\right)k_{sum}\sigma_i}{\omega_c^{2n+1}}\right|_{i=1} \\ \left.\dfrac{e_{sum}(0) + k_{sum}\sigma_i}{\omega_c^{n+1}}\right|_{i=2,\cdots,n} \end{cases} \\ &\leq \rho_i \end{aligned} \tag{4.52}$$

for all $t \geqslant T_5,\ i = 1, 2, \cdots, n$, where $\rho = \max\left\{\frac{e_{sum}(0)}{\omega_c^{n+1}} + \frac{k_{sum}\sigma}{\omega_c^n} + \frac{(1+\sum_{i=2}^{n} k_i)k_{sum}\sigma}{\omega_c^{2n+1}}, \frac{e_{sum}(0)+k_{sum}\sigma}{\omega_c^{n+1}}\right\}$. Q.E.D.

From the above, it is shown that, with plant dynamics largely unknown, the tracking error and its up to the $(n-1)^{st}$ order derivatives of the ADRC are bounded

and their upper bounds monotonously decrease with the observer and controller bandwidths.

4.3 Summary

The main result in this chapter is the analysis of the stability characteristics of the ESO, and the associated state feedback system ADRC. Both design scenarios, with and without a detailed mathematical model of the plant, are considered. It is shown that the asymptotic stability is assured for the dynamic system describing the estimation error and the closed-loop system in the former and boundedness of the errors in the later. Furthermore, it is demonstrated that the error upper bounds monotonously decrease with the observer and controller bandwidths.

CHAPTER V

A PRACTICAL APPROACH TO DISTURBANCE DECOUPLING CONTROL

In this chapter, a novel disturbance rejection based approach is proposed where the cross-couplings between control loops as well as external disturbances are treated as "disturbance," estimated in real time and rejected. This DDC strategy is rooted in the novel control method ADRC. Using the ESO as the observer, the new method requires very little information of the plant dynamics. The original concept of active disturbance rejection was proposed by Han [22]. The recently proposed new parameterization and tuning method greatly simplified the implementation of ADRC and made the design transparent to practicing engineers. More importantly, with the parameterized ADRC, it becomes a viable candidate for decoupling control.

As first shown in [81] for aircraft flight control and then in [82] for the jet engine problem, the ADRC is a natural solution to decoupling control problems in the presence of large uncertainties. In [81] and [82], the approach that they used still

needs the accurate matrix of the coefficients of the control signal, which is still demanding. Compared to the above problems, the dynamics of some industrial systems, such as chemical processes and MEMS gyroscopes, is even more nonlinear with less information available on how each input affects various outputs, which is needed to be known in the method used in [81, 82]. To address such challenges, an ADRC based DDC approach is proposed. With little modeling information assumed, namely the predetermined input-output paring, the decoupling problem is reformulated as that of disturbance rejection, where disturbance is defined as the cross channel interference. The effect of one input to all other outputs that it is not paired with is viewed as a disturbance to be rejected. In the ADRC framework, such disturbance is actively estimated using the ESO and canceled in the control law, in the absence of an accurate mathematical model of the plant.

The chapter is organized as follows. How a disturbance decoupling problem can be reformulated and solved as a disturbance rejection problem is shown in Section 5.1. The multi-loop ESO is shown in Section 5.2, followed by the disturbance decoupling controller design. Note that this chapter and the next chapter are the expanded version of [80].

5.1 Reformulation of Decoupling Control Problem

The ADRC is a relatively new control design concept. In this chapter, the ADRC based DDC approach is proposed to address the decoupling problem for systems with large uncertainties of the internal dynamics and significant unknown ex-

ternal disturbances. Let

$$\begin{aligned}
\vartheta_1 &= \left[y_1^{(n_1-1)}(t), y_1^{(n_1-2)}(t), \cdots, y_1(t)\right], \\
\vartheta_2 &= \left[y_2^{(n_2-1)}(t), y_2^{(n_2-2)}(t), \cdots, y_2(t)\right], \\
&\vdots \\
\vartheta_m &= \left[y_m^{(n_m-1)}(t), y_m^{(n_m-2)}(t), \cdots, y_m(t)\right], \\
u &= \left[u_1(t), u_2(t), \cdots, u_m(t)\right].
\end{aligned} \tag{5.1}$$

Consider a system formed by a set of coupled input-output equations with predetermined input-output parings

$$\begin{aligned}
y_1^{(n_1)} &= f_1\left(\vartheta_1, \vartheta_2, \cdots, \vartheta_m,\ u_2, u_3, \cdots, u_m, w_1\right) + b_{11}u_1 \\
y_2^{(n_2)} &= f_2\left(\vartheta_1, \vartheta_2, \cdots, \vartheta_m,\ u_1, u_3, \cdots, u_m, w_2\right) + b_{22}u_2 \\
&\vdots \\
y_m^{(n_m)} &= f_m\left(\vartheta_1, \vartheta_2, \cdots, \vartheta_m,\ u_1, u_2, \cdots, u_{m-1}, w_m\right) + b_{mm}u_m
\end{aligned} \tag{5.2}$$

where y_i is the output, u_i is the input, w_i is the external disturbances of the i^{th} loop, respectively, $y_i^{(n_i)}$ denotes the n_i^{th} order derivative of $y_i, i = 1, 2, \cdots, m$, and f_i represents the combined effect of internal dynamics and external disturbances in the i^{th} loop, including the cross channel interference. Note that $i = 1, 2, \cdots, m$ in the following. In (5.2), we assume that the numbers of inputs and outputs are the same; the orders n_i and the approximate values of b_{ii} are given.

A presumption in most existing decoupling control approaches is that an accurate mathematical model of the plant has been obtained. This could pose some rather considerable time and cost challenges in engineering practice. This is where the ADRC concept comes in. The idea is: if there is a viable alternative that allows us to realistically estimate f_i from input-output data, then the accurate mathematical description of f_i might not be required. It is the aim of this chapter to establish that the ESO is indeed a suitable solution for this task.

5.2 Multi-Loop Extended State Observer

Instead of identifying the plant dynamics off-line, we propose to estimate the combined effect of plant dynamics and external disturbance in real time. The idea is introduced as follows.

The square multivariable system (5.2) is an $m-$loop system. An ADRC based SISO controller is designed for each loop independently. Consider the i^{th} loop in (5.2)

$$y_i^{(n_i)} = f_i + b_{ii}u_i. \tag{5.3}$$

Let $x_{1,i} = y_i$, $x_{2,i} = \dot{y}_i, \cdots, x_{n_i,i} = y_i^{(n_i-1)}$ and $x_{n_i+1,i} = f_i$, which is added as an extended state. Assuming f_i is differentiable, define

$$h_i = \frac{df_i}{dt} = \dot{f}_i. \tag{5.4}$$

Then (5.3) can also be represented in state space form as

$$\begin{aligned}
\dot{x}_{1,i} &= x_{2,i} \\
&\vdots \\
\dot{x}_{n_i-1,i} &= x_{n_i,i} \\
\dot{x}_{n_i,i} &= x_{n_i+1,i} + b_{ii}u_i \\
\dot{x}_{n_i+1,i} &= h_i \\
y_i &= x_{1,i}
\end{aligned} \tag{5.5}$$

where $x_i = [x_{1,i}, x_{2,i}, \ldots, x_{n_i+1,i}]^T \in \mathbb{R}^{n_i+1}$, $u_i \in \mathbb{R}$, and $y \in \mathbb{R}$. An ESO for (5.5) is designed as

$$\begin{aligned}
\dot{\hat{x}}_{1,i} &= \hat{x}_{2,i} + l_{1,i}\left(x_{1,i} - \hat{x}_{1,i}\right), \\
&\vdots \\
\dot{\hat{x}}_{n_i-1,i} &= \hat{x}_{n_i,i} + l_{n_i-1,i}\left(x_{1,i} - \hat{x}_{1,i}\right), \\
\dot{\hat{x}}_{n_i,i} &= \hat{x}_{n_i+1,i} + l_{n_i,i}\left(x_{1,i} - \hat{x}_{1,i}\right) + b_{ii}u_i, \\
\dot{\hat{x}}_{n_i+1,i} &= l_{n_i+1,i}\left(x_{1,i} - \hat{x}_{1,i}\right)
\end{aligned} \tag{5.6}$$

where $\hat{x}_i = [\hat{x}_{1,i}, \hat{x}_{2,i}, \cdots, \hat{x}_{n_i+1,i}]^T \in \mathbb{R}^{n_i+1}$ and $[l_{1,i}, l_{2,i}, \cdots, l_{n_i,i}, l_{n_i+1,i}]^T$ are the observer gain parameters to be chosen. In particular, let us consider a special case where the gains are chosen as

$$[l_{1,i}, l_{2,i}, \cdots, l_{n_i,i}, l_{n_i+1,i}]^T = \left[\omega_{o,i}\alpha_{1,i}, \omega_{o,i}^2\alpha_{2,i}, \cdots, \omega_{o,i}^{n_i+1}\alpha_{n_i+1,i}\right]^T \tag{5.7}$$

with $\omega_{o,i} > 0$. Here $\alpha_{j,i}$, $j = 1, 2, \cdots, n_i + 1$ are chosen such that $s^{n_i+1} + \alpha_{1,i}s^{n_i} + \cdots + \alpha_{n_i,i}s + \alpha_{n_i+1,i}$ is Hurwitz. For simplicity, we just let $s^{n_i+1} + \alpha_{1,i}s^{n_i} + \cdots + \alpha_{n_i,i}s + \alpha_{n_i+1,i} = (s+1)^{n_i+1}$ where $\alpha_{j,i} = \frac{(n_i+1)!}{j!(n_i+1-j)!}$, $j = 1, 2, \cdots, n_i + 1$. It results in the characteristic polynomial of (5.6) to be

$$\lambda_{o,i}(s) = s^{n_i+1} + \omega_{o,i}\alpha_{1,i}s^{n_i} + \cdots + \omega_{o,i}^{n_i+1}\alpha_{n_i+1,i} = (s + \omega_{o,i})^{n_i+1}. \tag{5.8}$$

This makes $\omega_{o,i}$, which is the observer bandwidth of the i^{th} loop, the only tuning parameter for the i^{th} loop observer and the implementation process much simplified, compared to other observers. Generally, the larger the observer bandwidth, the more accurate the estimation. However, a large observer bandwidth will increase noise sensitivity. Therefore a proper observer bandwidth should be selected in a compromise between tracking performance and the noise tolerance.

5.3 Dynamic Disturbance Decoupling

With a well-tuned observer, the observer states will closely track the states of the augmented plant. By canceling the effect of f_i using $\hat{f}_i$, i.e, $\hat{x}_{n_i+1,i}$, the ADRC actively compensates for f_i in real time. The control law of the i^{th} loop is designed as follows. The ADRC control law is given by

$$u_i = \frac{k_{1,i}(r_i - \hat{x}_{1,i}) + \cdots + k_{n_i,i}(r_i^{(n_i-1)} - \hat{x}_{n_i,i}) - \hat{x}_{n_i+1,i} + r_i^{(n_i)}}{b_{ii}} \tag{5.9}$$

where r_i is the desired trajectory, and $k_{j,i}$, $j = 1, 2, \cdots, n_i$ are the controller gain parameters. The closed-loop system becomes

$$y_i^{(n_i)} = (f_i - \hat{x}_{n_i+1,i}) + k_{1,i}(r_i - \hat{x}_{1,i}) + \cdots + k_{n_i,i}(r_i^{(n_i-1)} - \hat{x}_{n_i,i}) + r_i^{(n_i)}. \quad (5.10)$$

Note that with a well-designed ESO, the first term in the right hand side (RHS) of (5.10) is negligible and the rest of the terms in the RHS of (5.10) constitute a PD controller with a feedforward term. Here $k_{j,i}$, $j = 1, 2, \cdots, n_i$ are the controller gain parameters selected to make $s^{n_i} + k_{n_i,i}s^{n_i-1} + \cdots + k_{1,i}$ Hurwitz. To further reduce the tuning parameters, all the controller poles are placed at $-\omega_{c,i}$. Then the approximate closed-loop characteristic polynomial becomes

$$\lambda_{c,i}(s) = s^{n_i} + k_{n_i,i}s^{n_i-1} + \cdots + k_{1,i} = (s + \omega_{c,i})^{n_i} \quad (5.11)$$

where $k_{j,i} = \frac{n_i!}{(j-1)!(n_i+1-j)!}\omega_{c,i}^{n_i+1-j}$, $j = 1, 2, \cdots, n_i$. This makes $\omega_{c,i}$, which is the controller bandwidth, the only tuning parameter for the i^{th} loop controller. The controller bandwidth is selected based on how fast and steady we want the output to track the set point. A large controller bandwidth generally increases the response speed but, pushed to the limit, it also could make the system oscillatory, or even unstable. Thus the controller bandwidth is tuned based on the competing requirements of performance and stability margin, together with noise sensitivity as well. In addition, a large controller bandwidth usually increases the magnitude and rate of change in control signal, and therefore the operation cost.

The primary reason for the above particular way of selecting $\alpha_{j,i}$ and $k_{j,i}$ is practicality: the observer and feedback gains must be easily tunable by the users. Another reason for such parameterization is that it reduces tuning to adjusting parameters that are familiar to engineers: bandwidth. It is advantageous that engineers could use a completely new design method without losing the critical insight gained from classical control: frequency response.

The proposed DDC approach renders a new alternative for decoupling control problems. The second key contribution of this dissertation is to present that the decoupling problems can be reformulated as a disturbance rejection one, without an elaborate plant model. In fact, the only information required is the orders of the subsystems associated with each input-output pair and the values of the corresponding input gains. Even when b_{ii} are unknown, the DDC method can still be implemented with the approximate b_{ii} as the tuning parameters [27]-[43]. Being able to deal with multivariable systems that have different orders for different input-output parings is another advantage of the proposed method. Overall, the DDC is a conceptually simple and easy to understand, and above all, practical solution for real world decoupling problems, where there is a large amount of uncertainties.

Since one loop of the DDC takes the coupling terms from other loops as disturbance, the stability analysis of ADRC presented in Chapter 4 also applies to the DDC. The stability analysis for the DDC has been presented in [80] and is omitted here to avoid redundancy.

5.4 Summary

In this chapter, a novel disturbance decoupling control method is proposed for a class of square multivariable systems of various orders. This is one of the main contributions of this dissertation. It is based on a novel disturbance rejection concept and it does not require an accurate mathematical model. The proposed DDC method is easy to understand and to implement, making it an appealing solution for practitioners. In addition, the parameter tuning guidance is given for the proposed DDC.

CHAPTER VI

DISTURBANCE DECOUPLING CONTROL IN CHEMICAL PROCESSES

In this chapter, two chemical process problems are investigated to show the effectiveness of the proposed DDC approach. The first example shows a linear multivariable system case, which is a refinery distillation column. The second one shows the nonlinear multivariable system case, which is a continuous stirred tank reactor (CSTR).

6.1 A Linear Multivariable System

A square multivariable system with two inputs and two outputs is illustrated how a linear MIMO system can be controlled by the proposed DDC framework. Distillation columns are very commonly used separation equipment in chemical and process industries. Figure 6 shows a simplified scheme of distillation column. A stream of mixture enters the column in the middle and two products exit. The light product is drawn from the top and the heavy product is obtained from the bottom.

The objective of the controller is to keep the purity of light product y_1 and the purity of heavy product y_2 at their desired values by manipulating the reflux flow rate u_1 and steam flow rate u_2. Generally, the feed flow rate is fixed. In case that the upstream process changes, the feed flow rate may have a disturbance. The Wood-Berry model

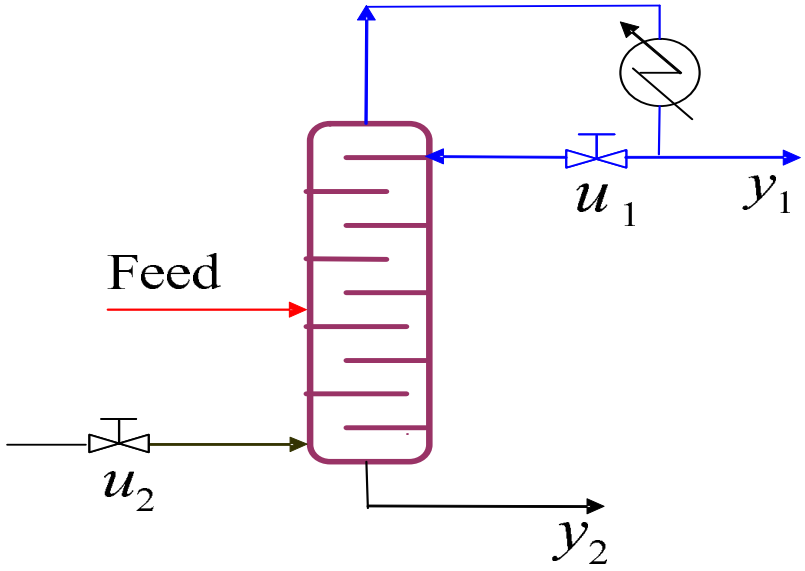

Figure 6: A simplified scheme of distillation column [29].

of a pilot-scale distillation column [29] with delay set to zero is considered, which is shown as below:

$$\begin{bmatrix} y_1(s) \\ y_2(s) \end{bmatrix} = \begin{bmatrix} \frac{K_{11}}{T_{11}s+1} & \frac{K_{12}}{T_{12}s+1} \\ \frac{K_{21}}{T_{21}s+1} & \frac{K_{22}}{T_{22}s+1} \end{bmatrix} \begin{bmatrix} u_1(s) \\ u_2(s) \end{bmatrix} \tag{6.1}$$

where $K_{11} = 12.8, K_{12} = -18.9, K_{21} = 6.6, K_{22} = -19.4, T_{11} = 16.7, T_{12} = 21,\ T_{21} = 10.9, T_{22} = 14.4$. The system (6.1) can be represented as

$$\begin{cases} \dot{y}_1(t) = f_1 + \dfrac{K_{11}}{T_{11}T_{12}} u_1(t) \\ \dot{y}_2(t) = f_2 + \dfrac{K_{22}}{T_{21}T_{22}} u_2(t) \end{cases} \tag{6.2}$$

which is the form of (5.2). Note f_1 and f_2 account for all other factors except u_1 and u_2 in loop 1 and loop 2 respectively.

6.1.1 Setpoint Tracking and Disturbance Rejection Performance

Let setpoints: $r_1 = 0,\ r_2 = 1$. unmeasured disturbances are added into the system as follows: $t = 0, d_1 = 0; t = 50, D(s) = \begin{bmatrix} \frac{K_{d1}}{T_{d1}s+1} \\ \frac{K_{d2}}{T_{d2}s+1} \end{bmatrix} d_2,\ t = 100, d_3 = 0$ where $K_{d1} = 3.8, K_{12} = 4.9, T_{d1} = 14.9, T_{d2} = 13.2, d_2 = 0.735$. The comparisons of disturbance rejection performance between the proposed DDC approach and the model predictive control (MPC) for Loop 1 and Loop 2 of the distillation column are shown in Figure 7 and Figure 8 respectively. Their respective design or tuning parameters are as below. The DDC parameters: $\omega_{c1} = \omega_{c2} = 0.2, \omega_{o1} = \omega_{o2} = 3$, $b_{0,11} = 0.8$, $b_{0,22} = -1.4$. Note that $b_{0,11}$ and $b_{0,22}$ are the approximate values of b_{11} and b_{22} in (6.2). The MPC parameters: model horizon: 120, sampling rate: 1 min, prediction horizon: 90, control move horizon: 30, output weightings: [1 1], and control weightings: [0.1, 0.1]. Figure 7 and Figure 8 show that the DDC achieves better performance than the MPC in disturbance rejection.

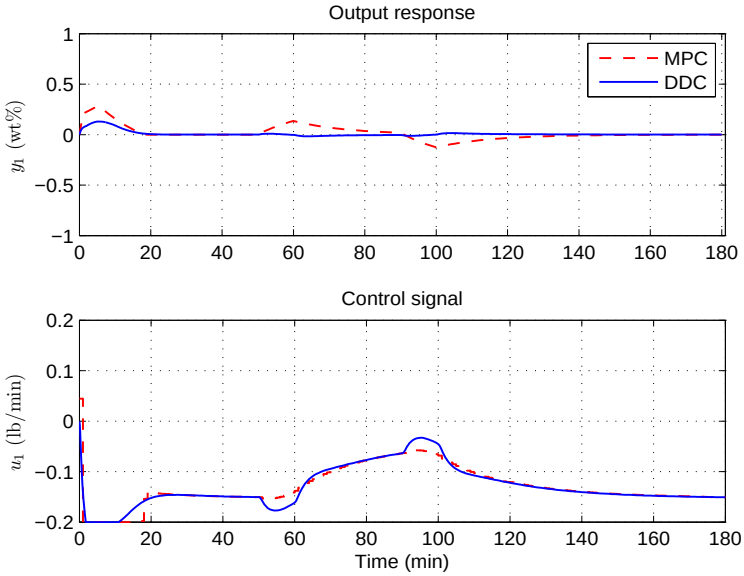

Figure 7: The comparison of disturbance rejection performance between the DDC and the MPC for Loop 1 of the distillation column.

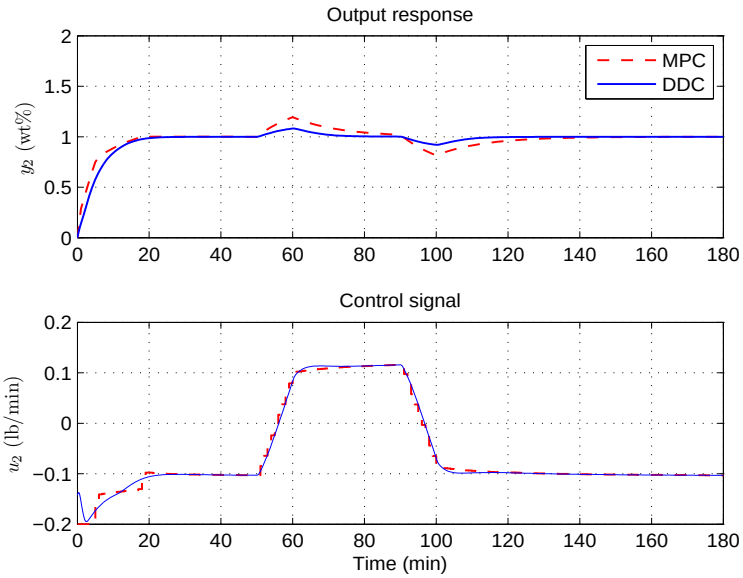

Figure 8: The comparison of disturbance rejection performance between the DDC and the MPC for Loop 2 of the distillation column.

6.1.2 Control Signal Selection

In practice, it is sometimes difficult to decide which control signal should be chosen for one specific loop in the absence of the plant model information. With the proposed DDC approach, this turns out not to be a problem. Consider the system

$$\begin{aligned} \dot{y}_1 &= f_1 + b_{11}u_1 + b_{12}u_2 \\ \dot{y}_2 &= f_2 + b_{21}u_1 + b_{22}u_2 \end{aligned} \tag{6.3}$$

with $b_{12} = 5b_{11}$, $b_{21} = 5b_{22}$, u_1 is the control signal of Loop 1, and u_2 is the control signal of Loop 2. That is, a clearly wrong choice was made regarding which input is the primary control signal for each loop. The output performance and control signal with the DDC are shown in Figure 9. It can be observed that the control signals for both loops become steep, but the systems can still be controlled to quickly go to the steady state.

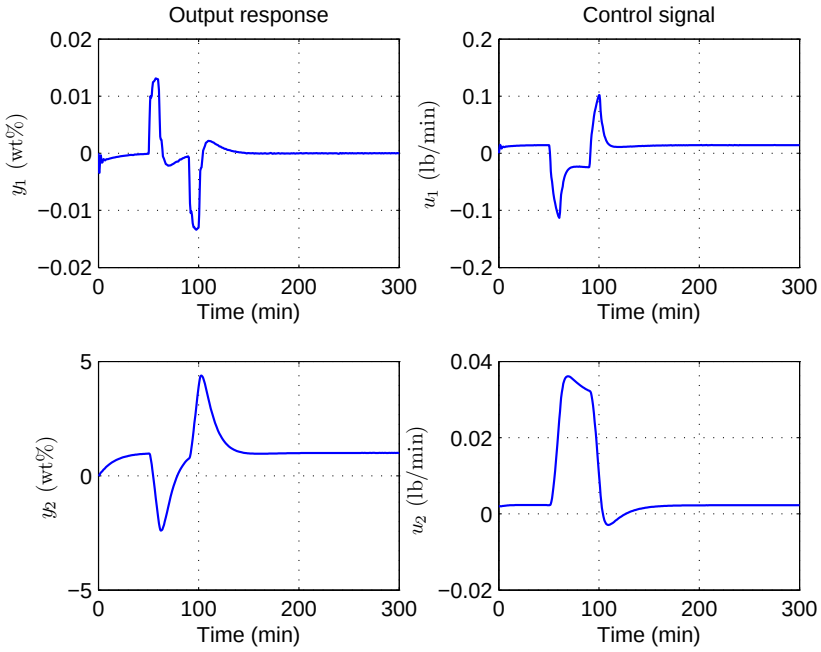

Figure 9: The performance with non-dominant control signal selection for each loop.

6.2 A Nonlinear Multivariable System

The continuous stirred tank reactor (CSTR) is widely used in chemical and process industries. Due to its highly nonlinear nature, it is a very important benchmark problem in process control. The system studied here is a CSTR with an irreversible exothermic first order reaction $A \rightarrow B$, which exhibits highly nonlinear characteristics [85]. Figure 10 shows the CSTR diagram. A pure stream of species A enters a constant volume reactor and a well-mixed stream of species A and B exit the reactor. The control objective is to keep the reactor concentration C_A and the reactor T temperature at their desired settings. The manipulated variables are the reactant feed flow rate F_{in} and the coolant water mass rate at the inlet F_w.

According to the reactant mass balance, reactor energy balance and the cooling jacket energy balance, a dynamic model of the plant is obtained. The plant model

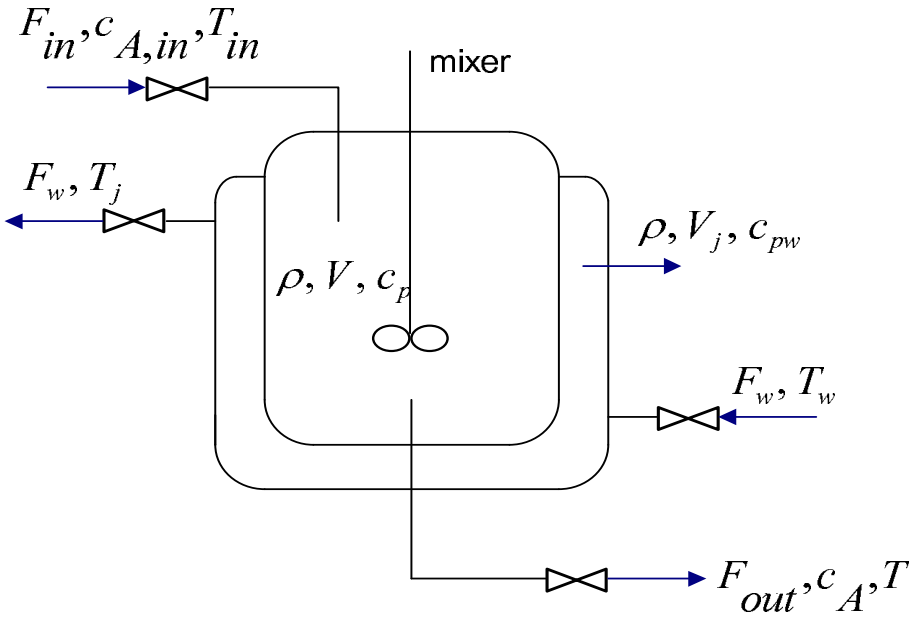

Figure 10: The CSTR diagram [87].

can be written into a standard nonlinear system representation as the following [87]:

$$\dot{x} = \begin{bmatrix} -rx_1 \\ \dfrac{-V \triangle Hrx_1 + UA(x_3 - x_2)}{V\rho C_p} \\ \dfrac{UA(x_2 - x_3)}{V_j \rho_w C_{pw}} \end{bmatrix} + \begin{bmatrix} \dfrac{C_{A,in} - x_1}{V} & 0 \\ \dfrac{T_{in} - x_2}{V} & 0 \\ 0 & \dfrac{T_w - x_3}{V_j \rho_w} \end{bmatrix} u \tag{6.4}$$

$$[y_1 \;\; y_2]^T = \begin{bmatrix} \dfrac{C_{A,in} - x_1}{C_{A,in}} & x_2 \end{bmatrix}^T$$

where

$$r = k_0 \exp(\frac{-E}{Rx_2}),$$

$$x = [x_1,\ x_2,\ x_3]^T = [C_A,\ T,\ T_j]^T,$$

$$u = [u_1,\ u_2]^T = [F_{in},\ F_w]^T.$$

The description of variables for this CSTR model is given in [87], which is also listed in Table I.

The output responses of CSTR under the control of the DDC are shown in Figure 11. The control signals of CSTR are shown in Figure 12. The tracking error of CSTR is shown in Figure 13. The design parameters for the DDC are: $b_{0,11} = -0.5, b_{0,22} = -0.03$. Note that $b_{0,11}$ and $b_{0,22}$ are the approximate values of b_{11}

Table I: Description of Variables for the CSTR Model [87]

Variable	Value	Unit	Description
F_{in}		$\mathrm{kg\,s^{-1}}$	The reactant feed flow rate
F_{out}		$\mathrm{kg\,s^{-1}}$	The outlet flow rate
V	1	$\mathrm{m^3}$	The volume of the tank reactor
c_A		$\mathrm{kg/m^3}$	The concentration of species A inside the tank
$c_{A,in}$	866	$\mathrm{kg/m^3}$	The concentration of species A at the feed
$c_{A,out}$		$\mathrm{kg/m^3}$	The concentration of species A at the outlet
k_0	4.10^8	$\mathrm{s^{-1}}$	Arrhenius rate constant
E	6.14	$\mathrm{Jmol^{-1}K^{-1}}$	Activation energy
R	8.314	$\mathrm{Jmol^{-1}K^{-1}}$	Gas law constant
T		K	Reactor temperature
ρ	866	$\mathrm{kgm^{-3}}$	Density of the reactant
C_p	1.791	$\mathrm{Jkg^{-1}K^{-1}}$	Specific heat capacity of species A and B
T_{in}	293	K	Temperature of the inlet stream
U	30	$\mathrm{Wm^{-2}K^{-1}}$	Overall heat transfer coefficient
A	50	$\mathrm{m^2}$	Heat transfer area
$\triangle\ H$	-140	$\mathrm{Jkg^{-1}}$	Heat of reaction
T_j		K	Temperature of the cooling jacket
V_j	0.2	$\mathrm{m^3}$	Volume of the cooling jacket
ρ_w	998	$\mathrm{kgm^{-3}}$	Density of the water
C_{pw}	4.181	$\mathrm{Jkg^{-1}K^{-1}}$	Specific heat capacity of water
F_w		$\mathrm{kgs^{-1}}$	Coolant water mass rate at the inlet and the outlet
T_w	290	K	Coolant water temperature at the jacket inlet

and b_{22} in (6.4). The two sets of tuning parameters for the DDC are: $\omega_{c1} = \omega_{c2} = 0.2, \omega_{o1} = \omega_{o2} = 0.03$. In addition, a reasonable amount of noise is added to the measurement in simulation. Compared to the signals, the noises are amount to about 1% and 0.1% in the two loops, respectively. The simulation results demonstrate that the nonlinear system is well controlled in the presence of cross-couplings and noises. The performance shows the effects of different controller and observer bandwidths. The larger observer bandwidths result in more accurate estimation, but it also leads to more sensitivity to noises. The larger controller bandwidths make the response faster, with a more jittery control signal.

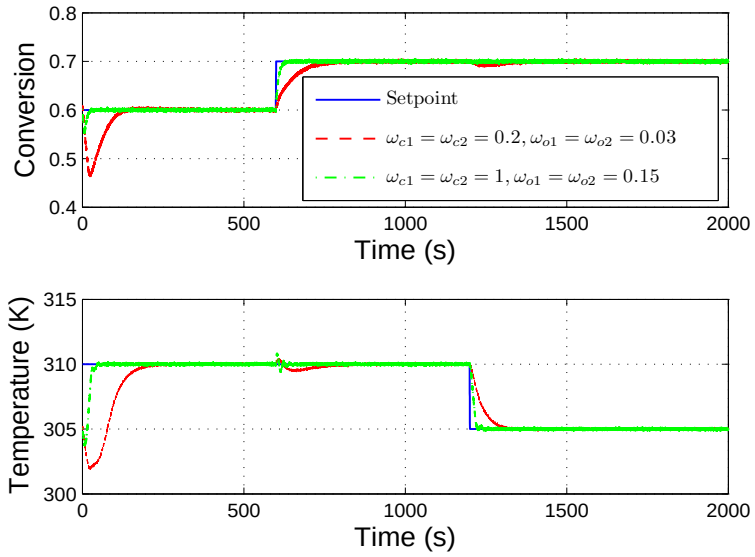

Figure 11: The output response of CSTR under the control of the DDC .

6.3 Summary

In this chapter, the proposed DDC method is applied to chemical process problems. Simulation results are quite promising. Excellent performance is attained in two case studies involving both the linear and nonlinear multivariable plants with significant uncertainties.

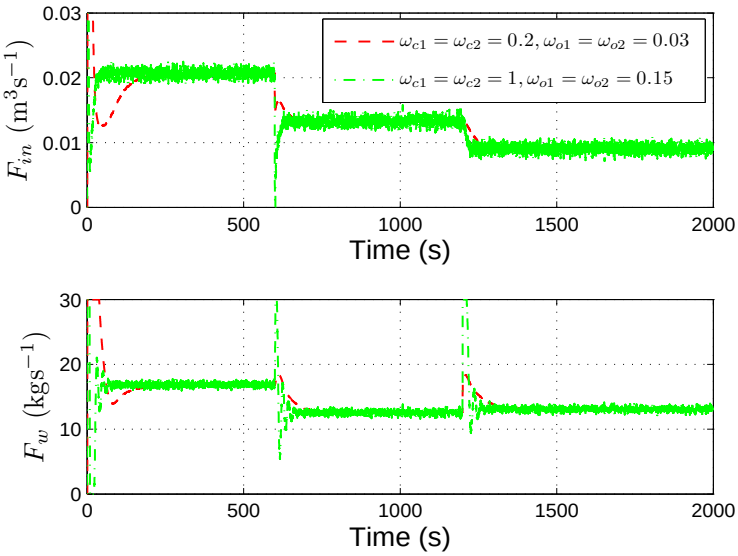

Figure 12: The control signals of CSTR.

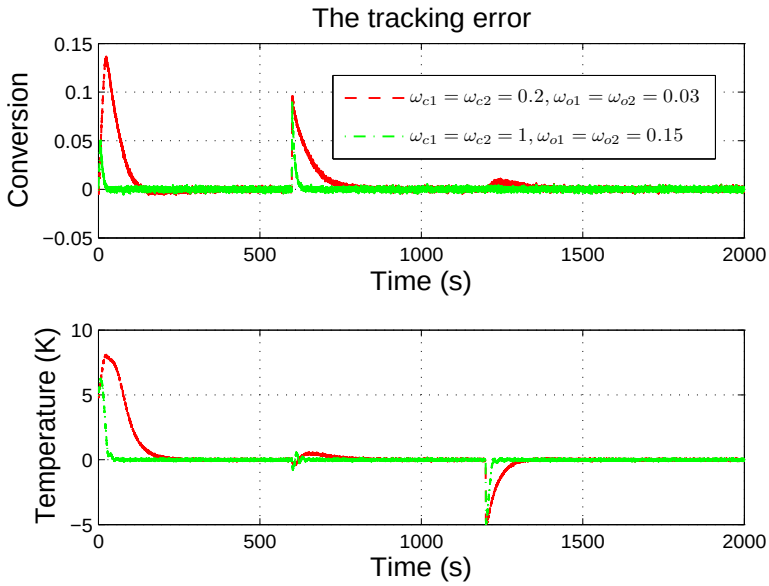

Figure 13: The tracking error of CSTR.

CHAPTER VII

CONTROL AND RATE ESTIMATION OF MEMS GYROSCOPES

There are two major control problems associated with vibrational MEMS gyroscopes: to control two vibrating modes (or axes) of the gyroscope, and to estimate a time-varying rotation rate. This chapter demonstrates how the DDC addresses these problems in the presences of the natural frequency mismatch between the two axes, mechanical-thermal noises, quadrature errors, and parameter variations. A demodulation approach based on the estimated dynamics of the system by the ESO is proposed to estimate the rotation rate. The simulation results on a Z-axis MEMS gyroscope show that the controller is very effective by driving the output of the drive axis to a desired trajectory, forcing the vibration of the sense axis to zero for a force-to-rebalance operation and precisely estimating the rotation rate.

This chapter is organized as follows. Section 7.1 introduces the background of MEMS gyroscopes. Section 7.2 describes the dynamics of MEMS gyroscopes. Section 7.3 presents how to apply the DDC to MEMS gyroscope control. Section 7.4

demonstrates how the time-varying rotation rate of MEMS gyroscopes is estimated using demodulation technique. Section 7.5 shows the simulation results. Finally, Section 7.6 summarizes this chapter. Note that Section 7.1 - Section 7.6 are extracted from [86][1].

7.1 Introduction to MEMS Gyroscopes

MEMS gyroscopes are inertial rate sensors batch fabricated on crystal silicon or polysilicon [88]. The operating principle of the MEMS gyroscopes is based on the energy transfer from driving mode to sensing mode of the gyroscopes caused by Coriolis acceleration. When the gyroscope is subject to a rotation rate, the response of the sensing mode provides the information of the rotation rate. With the advancement of MEMS technology, MEMS gyroscopes have been applied to automobiles for roll-over sensing and skid control, consumer electronics (for example, image stabilizations of cameras), GPS assisted inertial navigation, industry, aerospace, and so on [89]. However, fabrication imperfections and environmental variations produce undesirable coupling terms, unknown disturbances, input and measurement noises, frequency mismatch between two vibrating modes, and parameter variations which greatly degrade the performance of the gyroscopes. As a consequence, a control system is essential to improve the performance and stability of MEMS gyroscopes. Advanced control technologies should focus on exploiting the inherent structures of the vibratory MEMS gyroscopes, so as to achieve disturbance attenuation and performance robustness against modeling uncertainties.

Since the 1990's, there has been a limited amount of research on the control designs of MEMS gyroscopes. Most of the reported control approaches [90]-[96] assume constant rotation rates. However, in reality, the rotation rate is time varying.

[1] ©[2007] IEEE.

Little research is reported to estimate time-varying rotation rates. The design of the adaptive controller reported in [28] is based on the known states of the system dynamics. However, the velocity outputs of the two axes are unknown in practice. Furthermore, the multiple tuning parameters also make the adaptive controller very difficult to implement in real world situation. The controller in [97] assumes that the mechanical coupling terms are zeros. Actually the fabrication imperfections result in damping and stiffness coupling terms, which cause wrong measurement of the rotation rate. Hence, dealing with such time-varying uncertain dynamics of MEMS gyroscopes makes the control problem challenging and critically important. Since the system dynamics are only partially known, a solution that is insensitive to the uncertainties in system dynamics and is able to accurately determine the rotation rate is needed. In addition, the control solution should be practical and easy to implement.

In this chapter, the DDC is applied to control the MEMS gyroscope. In particular, the multi-loop ESO provides an estimate of the combination of the external disturbances and plant dynamics, which has modeling errors and structure uncertainties due to the unknown time varying rotation rate and the unknown quadrature error terms arising from mechanical imperfections. In addition, with the accurate estimate of the plant dynamics, an input time-varying rotation rate is accurately estimated with the demodulation technique.

7.2 Dynamics of MEMS Gyroscopes

We assume there is no coupling in the damping for both the drive and sense axes [94]. We allow for the frequency mismatch between the two axes. The governing

equations of the Z-Axis MEMS gyroscope [91] are represented by

$$\begin{aligned} \ddot{x} + 2\zeta\omega_n\dot{x} + \omega_n^2 x + \omega_{xy} y - 2\Omega\dot{y} &= \frac{K}{m} u_d(t) \\ \ddot{y} + 2\zeta_y\omega_y\dot{y} + \omega_y^2 y + \omega_{xy} x + 2\Omega\dot{x} &= \frac{K}{m} u_s(t) \end{aligned} \tag{7.1}$$

where $x\,(t)$ and $y\,(t)$ are drive axis and sense axis outputs respectively, ω_n and ω_y are natural frequencies of the drive and sense axes, ζ and ζ_y are damping coefficients, u_d and u_s are control inputs for the drive and sense axes, m is the proof mass, $2\Omega\dot{x}$ and $2\Omega\dot{y}$ are Coriolis accelerations, Ω is an unknown time-varying rotation rate, $\omega_{xy}y$ and $\omega_{xy}x$ are constant unknown quadrature error terms caused by stiffness couplings between two axes, and K is a constant that accounts for sensor, actuator, and amplifier gains. Note that there is a more elaborate model for MEMS gyroscopes [99], which should be used for controlling MEMS gyroscopes with time-varying rotation rate. The results obtained here is from a preliminary simulation with a simplified model.

Rotation sensing is achieved by forcing the drive axis into a fixed amplitude vibration, and measuring the displacement $y(t)$ of sense axis. We apply force-to-rebalance mode of operation onto the sense axis because of the general success of nulling-the-output approach in precise sensing applications [90]. In this mode, the output amplitude of the sense axis is continuously monitored and driven to zero, and the control signal becomes a part of measurement of rotation rate. Therefore our control tasks are to drive the drive axis to the desired trajectory with specified amplitude and resonant frequency, to force the output of the sense axis to zero, and to estimate the rotation rate in the presence of noises.

7.3 DDC for MEMS Gyroscopes

The existing control approaches for MEMS gyroscopes employ various methods to derive the accurate model of the plant. However, in practice, it is very challenging

to achieve precise model information. Especially for MEMS gyroscopes, the factors such as the mechanical-thermal noise, the measurement noise, the unknown time varying rotation rate, and the unknown quadrature error terms, bring modeling errors and structural uncertainties in the system. The mechanical imperfection and environmental variations also introduce the parameter variations to the model of MEMS gyroscopes. DDC is a natural fit for the MEMS gyroscope control due to its inherent disturbance rejection characteristics. How the idea of DDC can be applied to MEMS gyroscopes is briefly presented as follows.

The MEMS gyroscope can be understood as a coupled second-order system. The system (7.1) can be rewritten as

$$\begin{aligned} \ddot{x} &= -\left(2\zeta\omega_n\dot{x} + \omega_n^2 x + \omega_{xy} y - 2\Omega\dot{y}\right) + b_x u_d \\ \ddot{y} &= -\left(2\zeta_y\omega_y\dot{y} + \omega_y^2 y + \omega_{xy} x + 2\Omega\dot{x}\right) + b_y u_s \end{aligned} \tag{7.2}$$

where $b_x = b_y = \frac{K}{m}$.

Define

$$\begin{aligned} f_x &= -\left(2\zeta\omega_n\dot{x} + \omega_n^2 x + \omega_{xy} y - 2\Omega\dot{y}\right) \\ f_y &= -\left(2\zeta_y\omega_y\dot{y} + \omega_y^2 y + \omega_{xy} x + 2\Omega\dot{x}\right) \end{aligned} \tag{7.3}$$

where f_x and f_y are referred to as the generalized disturbance, or disturbance, because they represent both the unknown internal dynamics and the external disturbances of the drive and sense axes respectively. The couplings between the two axes are also taken as disturbances to each axis. Substituting (7.3) into (7.2), the system (7.2) becomes

$$\begin{aligned} \ddot{x} &= f_x + b_x u_d \qquad (a) \\ \ddot{y} &= f_y + b_y u_s. \qquad (b) \end{aligned} \tag{7.4}$$

The basic idea of the DDC is to obtain the estimated f_x and f_y, i.e., $\hat{f}_x$ and $\hat{f}_y$, and to compensate for them in the control law in real time. Note that the control designs of the drive and sense axes are the same and they are implemented in parallel.

For clarity, the concept of the DDC is explained with the control of the sense axis in the following. Let $\xi_{y1} = y$, $\xi_{y2} = \dot{y}$, $\xi_{y3} = f_y$ and $\xi_y = [\xi_{y1},\ \xi_{y2},\ \xi_{y3}]^T$. Assuming f_y is differentiable and the derivative of f_y ($h_y = \dot{f}_y$) is bounded, the state space form of (7.4b) is

$$\begin{aligned} \dot{\xi}_{y1} &= \xi_{y2} \\ \dot{\xi}_{y2} &= \xi_{y3} + b_y u_s \\ \dot{\xi}_{y3} &= h_y \\ y &= \xi_{y1}. \end{aligned} \tag{7.5}$$

An ESO for (7.5) is designed as

$$\begin{aligned} \dot{\hat{\xi}}_{y1} &= \hat{\xi}_{y2} + l_{y1}\left(\xi_{y1} - \hat{\xi}_{y1}\right) \\ \dot{\hat{\xi}}_{y2} &= \hat{\xi}_{y3} + l_{y2}\left(\xi_{y1} - \hat{\xi}_{y1}\right) + b_y u_s \\ \dot{\hat{\xi}}_{y3} &= l_{y3}\left(\xi_{y1} - \hat{\xi}_{y1}\right) \\ \hat{y} &= \hat{\xi}_{y1} \end{aligned} \tag{7.6}$$

where $L_y = [l_{y1},\ l_{y2},\ l_{y3}]^T$ is the observer gain. The observer gains are chosen such that the characteristic polynomial $s^3 + l_{y1}s^2 + l_{y2}s + l_{y3}$ is Hurwitz. For tuning simplicity, all the observer poles are placed at $-\omega_{oy}$. It results in the characteristic polynomial of (7.6) to be

$$\lambda_{oy}(s) = s^3 + l_{y1}s^2 + l_{y2}s + l_{y3} = (s + \omega_{oy})^3 \tag{7.7}$$

where ω_{oy} is the observer bandwidth of the sense axis and $l_{y1} = 3\omega_{oy}$, $l_{y2} = 3\omega_{oy}^2$, $l_{y3} = \omega_{oy}^3$. This makes ω_{oy} the only tuning parameter for the observer. Thus the implementation process of the observer is much simplified.

Once the observer is designed and well tuned, its outputs will track $y, \dot{y}, f_y$ respectively. By canceling the effect of f_y using $\hat{\xi}_{y3}$, the DDC actively compensates for f_y in real time. The control law is designed as follows. First, the control law

$$u_s = \frac{u_0 - \hat{\xi}_{y3}}{b_y} \tag{7.8}$$

approximately reduces the original plant (7.4b) to

$$\ddot{y} \approx u_0 \tag{7.9}$$

which is a much simple control problem to deal with. A simple controller can be designed as

$$u_0 = k_{y1}(r_y - \hat{\xi}_{y1}) + k_{y2}(\dot{r}_y - \hat{\xi}_{y2}) + \ddot{r}_y \tag{7.10}$$

where r_y is the desired trajectory of the sense axis. Note that a feedforward mechanism is employed in (7.10) for the purpose of reducing the tracking error. The controller gains are selected so that the closed-loop characteristic polynomial $s^2 + k_{y2}s + k_{y1}$ is Hurwitz. For tuning simplicity, all the controller poles are placed at $-\omega_{cy}$. Then the approximate closed-loop characteristic polynomial is

$$\lambda_{cy}(s) = s^2 + k_{y2}s + k_{y1} = (s + \omega_{cy})^2 \tag{7.11}$$

where $k_{y1} = \omega_{cy}^2$, $k_{y2} = 2\omega_{cy}$. This makes ω_{cy}, the controller bandwidth, the only tuning parameter for the controller of the sense axis.

7.4 Rotation Rate Estimation

Considering the sense axis of the MEMS gyroscope system, both Coriolis acceleration and quadrature error terms are amplitude modulated signals centered at the resonant frequency of the drive axis. The only distinguishing characteristic between the two signals is that they have a relative phase shift of 90°. Therefore we can take advantage of this characteristic to separate the undesired quadrature errors from the useful Coriolis acceleration through the demodulation technique.

Applying the ESO (7.6) and the control law (7.8) and (7.10) to the MEMS gyroscope, we can drive the output of the drive axis x to the desired trajectory r_x with ideal amplitude and resonant frequency, force the output of sense axis y to zero,

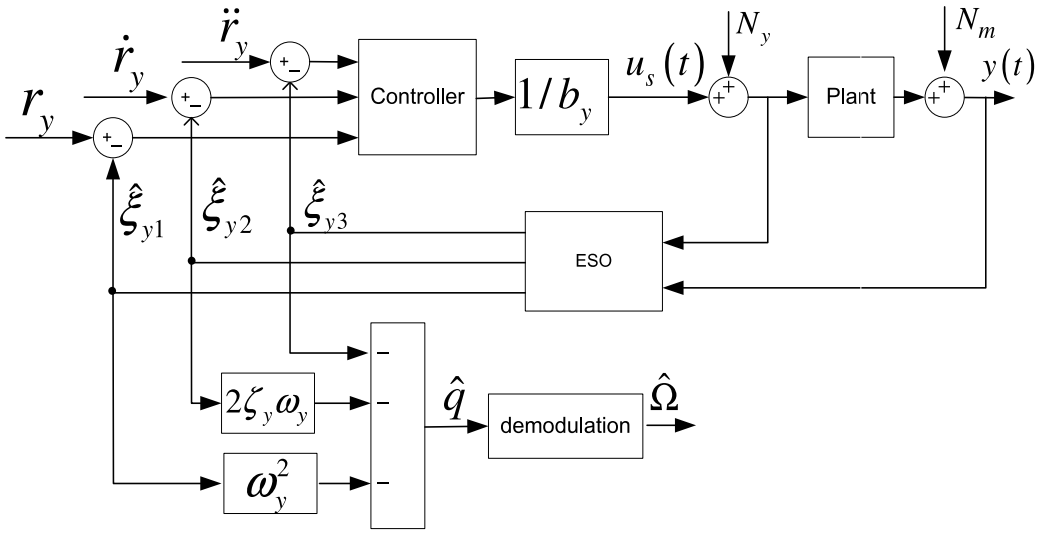

Figure 14: Block diagram of the ADRC and rate estimation.

and accurately estimate the states of the drive and sense axes. Based on the accurate state estimation and the good tracking of the drive and sense axes, the rotation rate is determined. The block diagram of the ADRC for the sense axis control and rate estimation is shown in Figure 14, where a demodulation block is used for the estimation of rotation rate. In Figure 14, N_y represents the mechanical-thermal noise input to the sense axis and N_m represents the measurement noise (position noise) at the output of the sense axis [94].

The desired trajectory of the drive axis is $r_x = A\cos(\omega t)$. With the ideal tracking of the ADRC, we have $x = r_x = A\cos(\omega t)$, and $\dot{x} = -A\omega\sin(\omega t)$. From (7.3), we have

$$\omega_{xy}x + 2\Omega\dot{x} = -\left(f_y + 2\zeta_y\omega_y\dot{y} + \omega_y^2 y\right). \tag{7.12}$$

Let $q = \omega_{xy}x + 2\Omega\dot{x}$. It is assumed that the rotation rate is a sinusoidal signal [94], and $\Omega = \Omega_0\sin(2\pi f_{\text{rate}}t)$ where Ω_0 and $2\pi f_{\text{rate}}$ are amplitude and angular frequency

of the rate. Then we have

$$\begin{aligned} q\sin(\omega t) &= (\omega_{xy}x + 2\Omega\dot{x})\sin(\omega t) \\ &= \omega_{xy}A\cos(\omega t)\sin(\omega t) - 2\Omega A\omega\sin^2(\omega t) \\ &= \frac{1}{2}\omega_{xy}A\sin(2\omega t) - 2\Omega A\omega\frac{1-\cos(2\omega t)}{2} \\ &= \frac{1}{2}\omega_{xy}A\sin(2\omega t) + \Omega A\omega\cos(2\omega t) - \Omega A\omega \end{aligned} \tag{7.13}$$

where $\omega \gg 2\pi f_{\text{rate}}$ in the MEMS gyroscopes. In (7.13), the high frequency signals $\frac{1}{2}\omega_{xy}A\sin(2\omega t)$ and $\Omega A\omega\cos(2\omega t)$ will be filtered out through a low pass filter (LPF). Therefore the rotation rate Ω can be demodulated from the signal q by multiplying $\sin(\omega t)$ and dividing by a gain introduced from modulation/demodulation, and filtering the resultant signal with a LPF, that is

$$\Omega = F_{\text{LPF}}\left(-\frac{q\sin(\omega t)}{A\omega}\right) \tag{7.14}$$

where $F_{\text{LPF}}(.)$ represents the function of the LPF. With the information of the ESO, according to (7.12), the signal q in (7.14) can be estimated as follows

$$\hat{q} = -\left(\hat{f}_y + 2\zeta_y\omega_y\hat{\xi}_{y2} + \omega_y^2\hat{\xi}_{y1}\right). \tag{7.15}$$

The rotation rate can be estimated by

$$\hat{\Omega} = F_{\text{LPF}}\left(-\frac{\hat{q}\cdot\sin(\omega t)}{A\omega}\right). \tag{7.16}$$

The transfer function of the low-pass filter is chosen as

$$G_{\text{LPF}}(s) = \frac{1}{(\tau s+1)^2} \tag{7.17}$$

where τ is the time constant of the filter.

7.5 Simulation Results

A control system based on the DDC is designed and simulated on a model of the Berkeley Z-axis gyroscope [98]. The key parameters are $\omega_n = 81681.4$ rad/sec,

K=0.8338, $\omega_y = 80864.6$ rad/sec, $\zeta = 4.5455 \times 10^{-5}, \zeta_y = 3.125 \times 10^{-4}, \omega_{xy} = 6000$ rad^2/sec^2, and $m = 2 \times 10^{-9}$ kg. The design parameters $b_x = b_y = \frac{K}{m} = 4.169 \times 10^8$. The actual rotation rate is assumed to be a sinusoidal signal $\Omega = 0.1\sin(2\pi \mathrm{f}_{\mathrm{rate}} t)$ and $f_{\mathrm{rate}} = 50$ Hz. The reference signal for the drive axis is $r_x = A\cos(\omega t)$, where $\omega = 84194.7$ rad/sec. Typically $A = 10^{-6}$ m. We use $A = 50$ in "simulation units" to represent this [90]. The reference signal of the sense axis is $r_y = 0$. In the simulation, the mechanical-thermal noise is added to the drive axis, and the mechanical-thermal noise as well as the measurement noise is added to the sense axis. The PSD of mechanical-thermal noise for the drive axis is 2.4×10^{-28} N^{2}sec, and the one for the sense axis is 1.63×10^{-27} N^{2}sec. The PSD of measurement noise for the sense axis is 1.49×10^{-27} N^{2}sec [94]. The controller and observer parameters for the drive axis are: $\omega_{cx} = 4.95 \times 10^5$ rad/sec, $\omega_{ox} = 2.45 \times 10^6$ rad/sec. The controller and observer parameters for the sense axis are: $\omega_{cy} = 5 \times 10^5$ rad/sec, $\omega_{oy} = 2 \times 10^7$ rad/sec. The time constant of LPF is $\tau = 6.7 \times 10^{-5}$ sec.

The output of the drive axis under the control of the DDC is shown in Figure 15. After approximate 1 ms, the amplitude of the drive axis is maintained at 50 as desired, and the frequency of the drive axis is driven to the resonant frequency ω as expected. The output of the sense axis under the control of the DDC is shown in Figure 16. The stabilized output is around 0.01% of the uncontrolled amplitude of y, which shows that the sense axis is driven to almost zero. The rotation rate estimation at $\mathrm{f}_{\mathrm{rate}} = 50$ Hz is shown in Figure 17. The control signals of the drive and sense axes are shown in Figure 18. It is implemented through FPGA. The estimated rotation rate can track the actual rotation rate after approximate 2.5 ms and the steady-state peak error is about 1% of the actual rotation rate magnitude. Compared to the performance that was obtained by using the adaptive control in [92], this demonstrates that a fast and accurate estimation of the rotation rate is achieved.

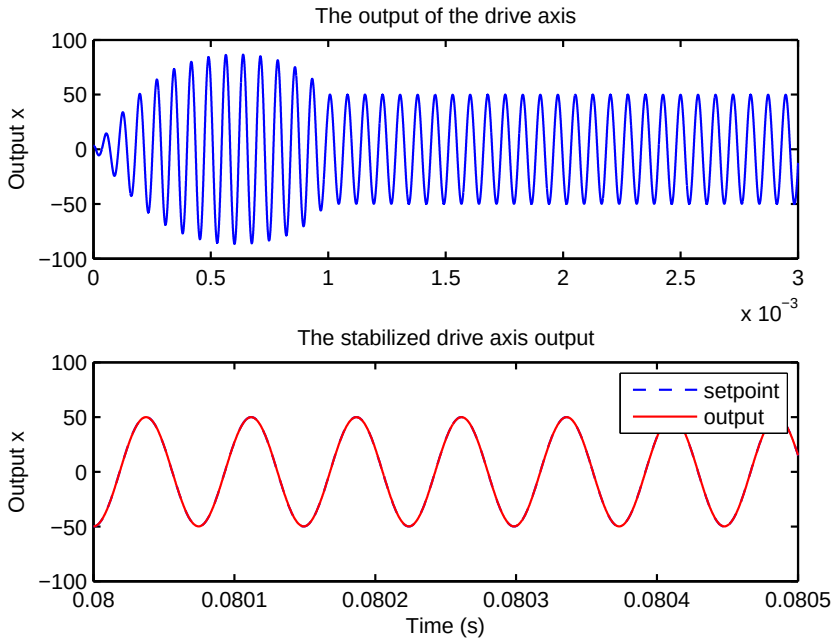

Figure 15: The output of the drive axis.

To further investigate the robustness of DDC against parameter variations, the system parameters are changed as follows: the natural frequency of the drive axis ω_n is increased by 10%, the natural frequency of the sense axis ω_y is increased by 20%, and the magnitude of the quadrature error term is increased by 20%. With the plant parameter variations, the output of the drive axis, the output of the sense axis, and the rotation rate estimation are shown in Figs. 19-21, respectively. Note that the tuning parameters of the DDC and the rate frequency are not changed. The rotation rate estimations at f_{rate} = 100 Hz and f_{rate} = 200 Hz are shown in Figure 22 and Figure 23 respectively, without changing the parameters of the DDC and the LPF. With f_{rate} = 100 Hz and f_{rate} = 200 Hz, the estimated rotation rates can track the actual rotation rate after approximate 2.5 ms and the steady state peak errors are about 1% of the amplitude of actual rotation rate. Compared to the performance that was obtained by using the adaptive control in [92], the above simulation shows the strong robustness of the DDC.

The simulation and hardware implementation results for MEMS gyroscope

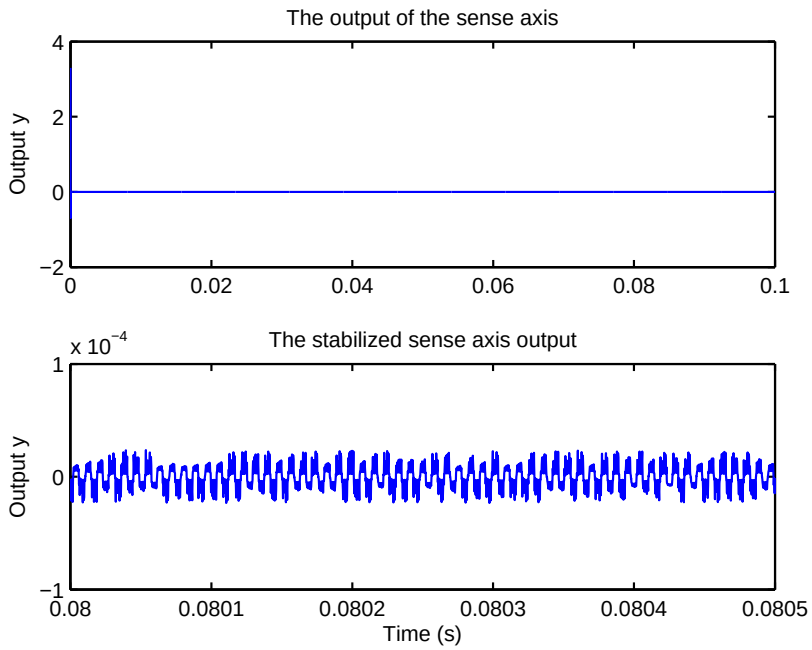

Figure 16: The output of the sense axis.

control with the discrete ADRC are presented in [100, 101].

7.6 Summary

In this chapter, the DDC approach is used to control the drive and sense axes of a vibrational MEMS gyroscope. Based on the accurate estimation of the internal plant dynamics and external disturbances of the multi-loop ESO, a demodulation technique is used to estimate the time-varying rotation rate. Since the DDC does not require an accurate mathematical model of the plant, it is very effective for controlling the MEMS gyroscope and estimating the time-varying rotation rate in the presence of noises and parameter variations. Compared to the performance that was obtained by using the adaptive control in [92], the simulation results demonstrated the high tracking performance and robustness of the DDC, as well as the fast and accurate estimation of the input time-varying rotation rate. Since most MEMS sensors have similar control problems to MEMS gyroscopes, i.e. precise amplitude and frequency

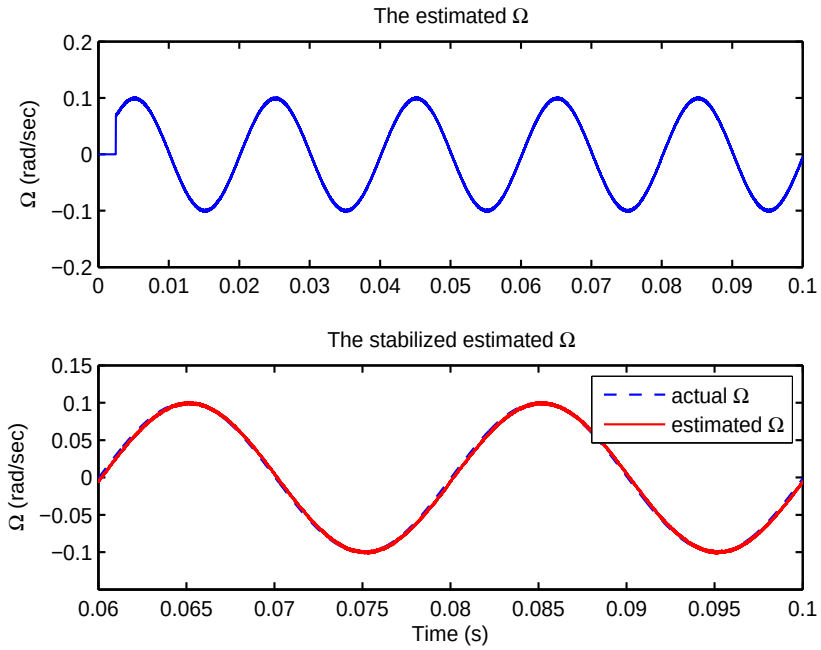

Figure 17: The rotation rate estimation at $f_{rate} = 50$ Hz.

control, disturbance rejection, and minimizing the effects of fabrication imperfection, the DDC provides a new solution to the problems. The applications of the DDC are expected to be broadened to other MEMS sensors such as micro-accelerometers and pressure sensors.

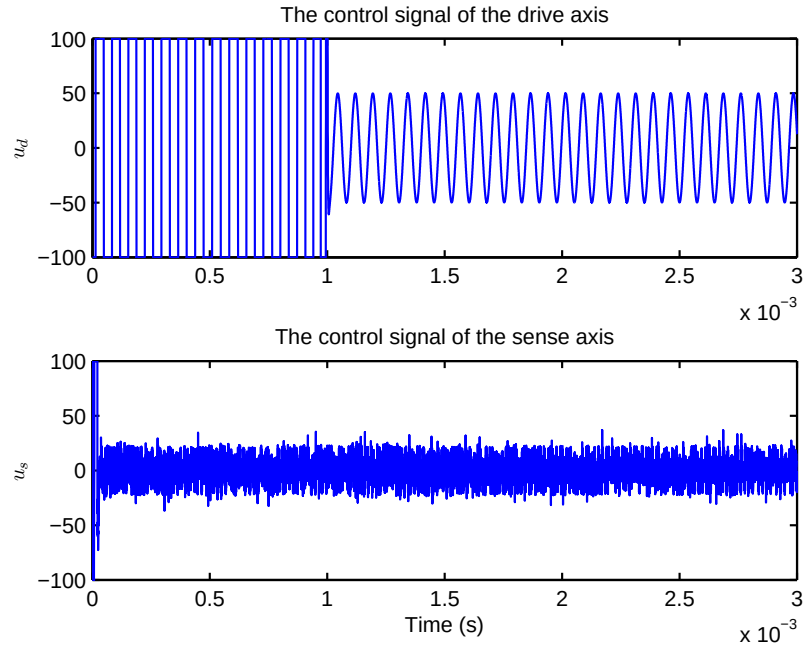

Figure 18: The control signals of the drive and sense axes.

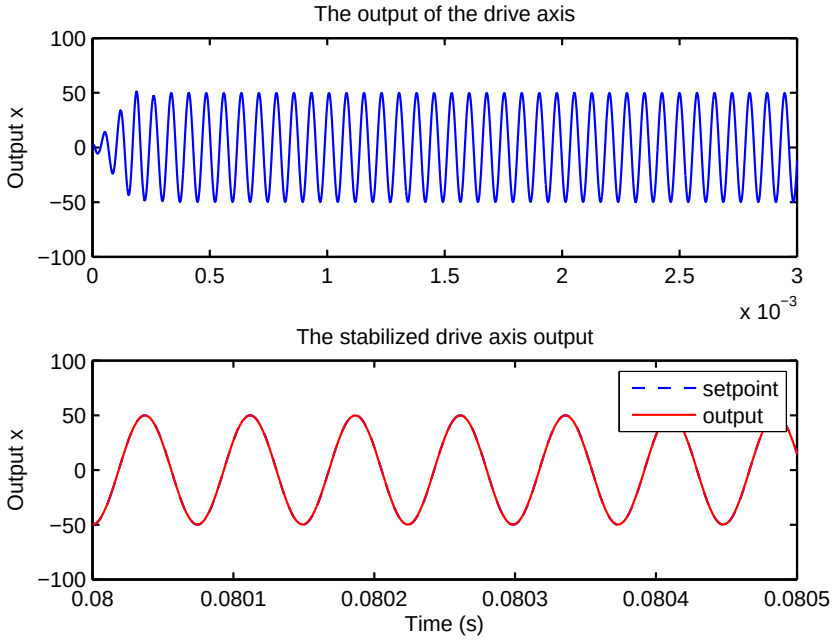

Figure 19: The output of the drive axis with parameter variations.

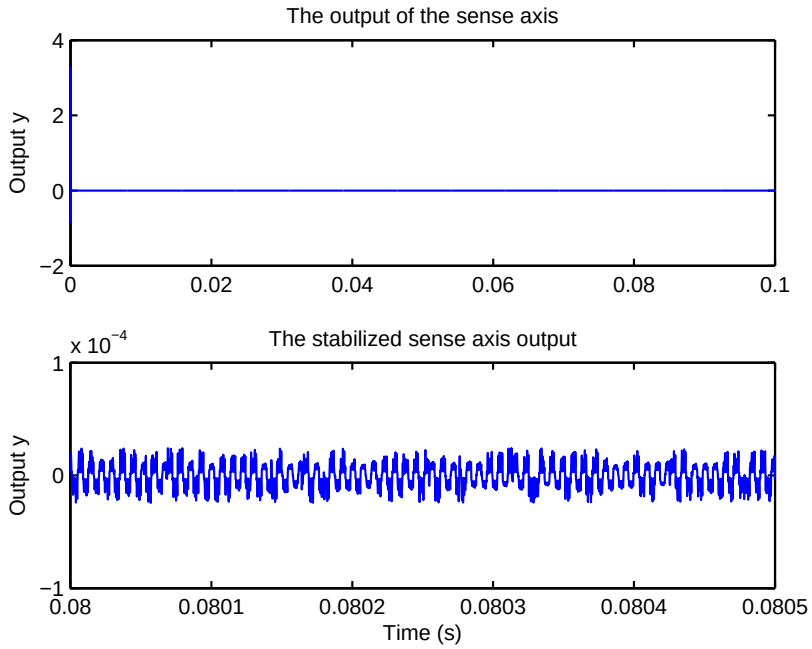

Figure 20: The output of the sense axis with parameter variations.

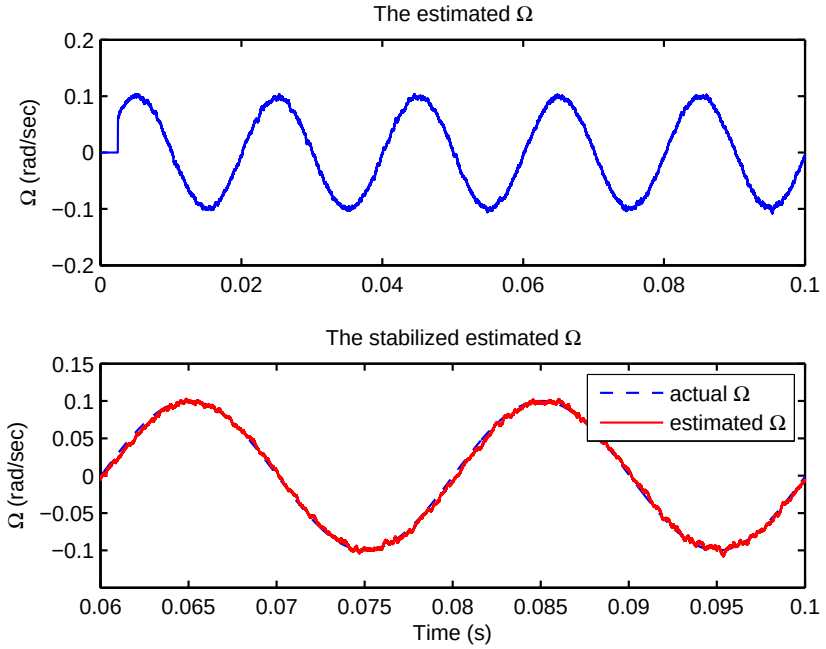

Figure 21: The rotation rate estimation at $f_{rate} = 50$ Hz with parameter variations.

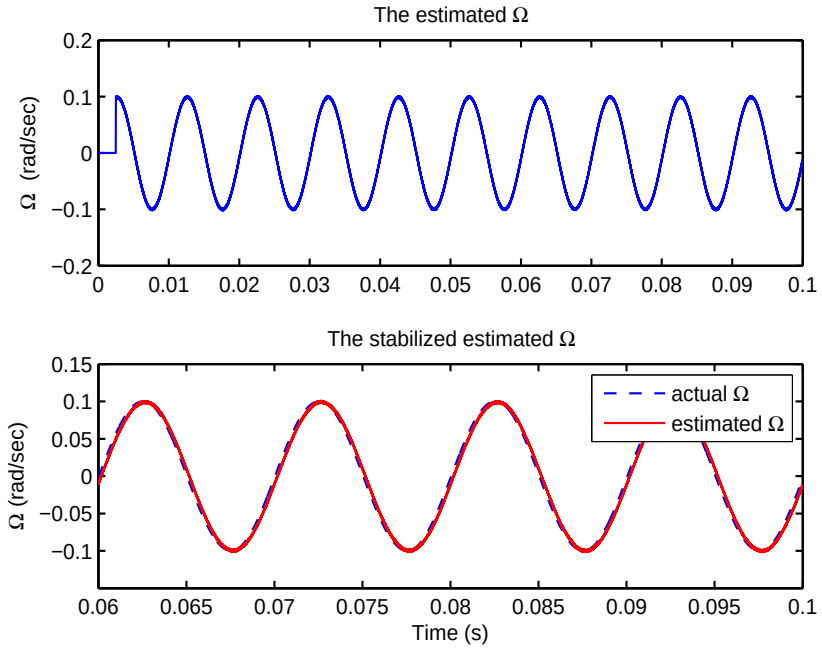

Figure 22: The rotation rate estimation at $f_{rate} = 100$ Hz.

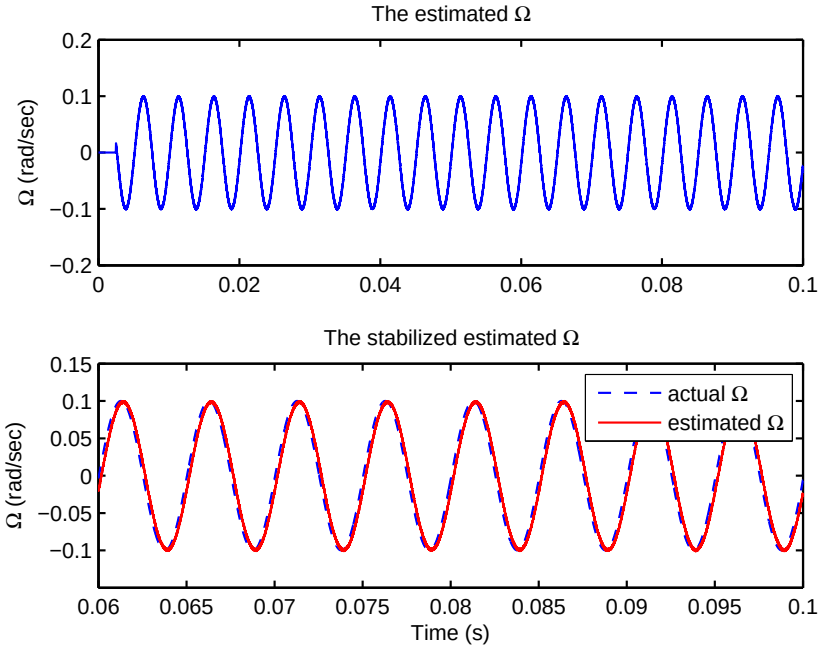

Figure 23: The rotation rate estimation at $f_{rate} = 200$ Hz.

CHAPTER VIII

CONCLUDING REMARKS

8.1 Findings and Conclusions

One main result in this dissertation is the analysis of the convergence and the stability characteristics of the ESO and the associated compensation system, ADRC. It is demonstrated that, for a large class of physical processes, both the unknown plant dynamics and external disturbances can be estimated using the unique state observer, ESO. Both design scenarios, with and without a detailed mathematical model of the plant, are considered. It is shown that the asymptotic stability is assured for the dynamic system describing the estimation error and the closed-loop system when the plant mathematical model is given. For the other case, i.e., without a mathematical model of the plant, it is shown that the observer estimation error, the closed-loop tracking error, and its up to the $(n-1)^{st}$ order derivatives are shown to be bounded. Furthermore, it is demonstrated that the observer estimation error upper bound monotonously decreases with the observer bandwidth and the closed-loop tracking error upper bound monotonously decreases with the bandwidths of the

observer and the controller. The results in this dissertation solidify the foundation for the alternative control design paradigm, ADRC, one that is not bound by the prevailing notion that an accurate mathematical description of the physical process is required. The analytical study is furthered supported by both the simulation and experimental results, showing that the plant dynamics and disturbance can be realistically estimated in real time based on the plant input-output data and some limited knowledge of the plant structure and order.

The other main contribution of this dissertation is the formulation of the DDC approach for a class of square multivariable systems of various orders, based on the disturbance rejection nature of the ADRC. It does not require an accurate mathematical model. The proposed DDC method is easy to understand and to implement, making it an appealing solution for practitioners. Because of the simplicity of the proposed DDC for implementation, it has been successfully simulated in chemical processes and MEMS gyroscopes. Simulation results are quite promising. Through comparing the DDC performance with MPC performance in chemical process problems and adaptive control performance in MEMS gyroscopes, DDC achieves high performance in tracking, disturbance rejection, and robustness in the chemical processes and MEMS gyroscopes involving both the linear and nonlinear multivariable plants with significant uncertainties.

8.2 Remarks on Future Research

Based on the work of this dissertation, further investigation could be divided into theoretical part and application part.

From the theoretical side, future research could be to focus on the following directions. First, the stability analysis of the ADRC has some assumptions for the two cases: with the plant model information and without the plant model information.

With relaxing the limitation of the stability analysis in this dissertation, what conclusions will be obtained for the stability characteristics of the ESO and the ADRC? Second, the coefficient of the control signal and the order of the system in the current ADRC framework still need to be known in order to design the control system. What can be achieved for the control system design without the above information? In other words, what approach can be developed for systems with time-varying coefficients of control signals and/or systems without order information? Third, the DDC is proposed for square multivariable systems without time delay. How to develop a new approach to design the control system for non-square multivariable systems and /or for MIMO systems with time delay, under the ADRC framework?

From the application side, future investigation could be conducted with the following possible directions. The DDC is a very practical approach and has not been widely applied to real systems. The applications of the DDC to large scale systems are very interesting. For example, energy and environmental control issues are currently one society's main concern. The DDC is a good approach to energy and environmental control problems, since it is hard to provide a mathematical model.

These are interesting topics that could be further investigated.

BIBLIOGRAPHY

[1] G. Basile and G. Marro, "On the observability of linear, time-invariant systems with unknown inputs, *Journal of Optimization Theory and Applications*, vol. 2, no. 6, pp. 410-415, 1969.

[2] C. Johnson, "Accommodation of external disturbances in linear regulator and servomechanism problems," *IEEE Transactions on Automatic Control*, vol. AC-16, no. 6, pp. 635-644, 1971.

[3] G. Hostetter and J. Meditch, "On the generalization of observers to systems with unmeasurable, unknown inputs," *Automatica*, vol. 9, pp. 721-724, 1973.

[4] C. Johnson, "Theory of disturbance-accommodating controllers,", *Control and Dynamic Systems*, vol. 12, pp. 387-489, 1976.

[5] V. Gourishangkar, P. Kudva, and K. Ramar, "Reduced-order observers for multivariable systems with inaccessible disturbance inputs," *International Journal of Control*, vol. 25, pp.311-319, 1977.

[6] P. C. Muller, "Indirect measurements of nonlinear effects by state observers," *Proc. IUTAB Symposium Nonlinear Dynamics in Engineering Systems*, pp. 205-215, 1990.

[7] J. Profeta, W. Vogt, and M. Mickle, "Disturbance estimation and compensation in linear systems," *IEEE Transaction on Aerospace and Electronic Systems*, vol. 26, no. 2, pp. 225-231, 1990.

[8] J. Chen, R. J. Patton, and H. Zhang, "Design of unknown input observers and

robust fault detection filters," *International Journal of Control*, vol. 63, no. 1, pp. 85-105, 1995.

[9] T. Umeno, and Y. Hori, "Robust speed control of DC servo motors using modern two degrees-of-freedom controller design," *IEEE Transactions on Industrial Electronics*, vol. 38, pp. 363-368, 1991.

[10] Y. Hori, K. Shimura, and M. Tomizuka, "Position/force control of multi-axis manipulator based on the TDOF robust servo controller for each joint," *Proc. of the American Control Conference ACC/WM9*, vol. 1, pp. 753-757, 1992.

[11] H. Lee and M. Tomizuka, "Robust motion controller design for high-accuracy positioning systems," *IEEE Transactions on Industrial Electronics*, vol. 43, pp. 48-55, 1996.

[12] T. Mita, M. Hirata, K. Murata, and H. Zhang, "H_∞ control versus disturbance-observer-based control," *IEEE Transactions on Industrial Electronics*, vol. 45, no. 3, pp. 488-495, 1998.

[13] R. Bickel and M. Tomizuka, "Passivity-based versus disturbance observer based robot control: equivalence and stability," *ASME Journal of Dynamics Systems, Measurement, and Control*, vol. 121, pp. 41-47, 1999.

[14] E. Schrijver and J. van Dijk,"Disturbance observers for rigid mechanical systems: Equivalence, stability, and design," *ASME Journal of Dynamics Systems, Measurement, and Control*, vol. 124, no. 4, pp. 539-548, 2002.

[15] Y. Choi, K. Yang, W. K. Chung, H. R. Kim, and I. H. Suh, "On the robustness and performance of disturbance observers for second-order systems," *IEEE Transactions on Automatic Control*, vol. 48, no. 2, pp. 315-320, 2003.

[16] K. Yang, Y. Choi, and W. Chung, "On the tracking performance improvement of optical disk drive servo systems using error-based disturbance observer," *IEEE Transactions on Industrial Electronics*, vol. 52, no. 1, pp. 270-279, 2005.

[17] S. Kwon and W. K. Chung, "Robust performance of the multiloop perturbation compensator," *IEEE/ASME Transaction on Mechatron.*, vol. 7, no. 2, pp. 190-200, 2002.

[18] S. Kwon and W. K. Chung, "A discrete-time design and analysis of perturbation observer for motion control applications," *IEEE Transactions on Control Systems Technology*, vol. 11, no. 3, pp. 399-407, 2003.

[19] S. Kwon and W. K. Chung, "Combined synthesis of state estimator and perturbation observer," *ASME Journal of Dynamic Systems, Measurement, and Control*, vol. 125, pp. 19-26, 2003.

[20] S. Kwon, "Robust kalman filtering with perturbation estimation process," *Proc. of the American Control Conference*, pp. 997-1002, 2006.

[21] Z. Gao, "Active disturbance rejection control: a paradigm shift in feedback control system design," *Proc. of the American Control Conference*, pp. 2399-2405, 2006.

[22] J. Han, "A class of extended state observers for uncertain systems," *Control and Decision*, vol. 10, no. 1, pp. 85-88, 1995. (In Chinese)

[23] J. Han, "Nonlinear state error feedback control," *Control and Decision*, vol. 10, no. 3, pp. 221-225, 1995. (In Chinese)

[24] J. Han, "Auto-disturbance rejection control and its applicationss," *Control and Decision*, vol. 13, no. 1, pp. 19-23, 1998. (In Chinese)

[25] J. Han, "Nonlinear design methods for control systems," *Proc. of the 14th IFAC World Congress*, 1999.

[26] Z. Gao, Y. Huang, and J. Han, "An alternative paradigm for control system design," *Proceedings of IEEE conference on Decision and Control*, pp. 4578-4585, 2001.

[27] Z. Gao, "Scaling and parameterization based controller tuning," *Proceedings of the American Control Conference*, pp. 4989-4996, 2003.

[28] L. Dong and R.P. Leland, "The adaptive control system of a MEMS gyroscope with time-varying rotation rate," *Proceedings of the American Control Conference*, pp. 3592-3597, 2005.

[29] R. K. Wood and M.W. Berry, "Terminal composition control of a binary distillation Column," *Chemical Engineering Science*, vol. 28, pp. 1707-1717, 1973.

[30] R. Brockett, "New Issues in the Mathematics of Control," *Mathematics Unlimited - 2001 and Beyond*, B. Engquist and W. Schimid Ed., pp. 189-220, Springer, 2001.

[31] Y. X. Su, B. Y. Duan, C. H. Zheng, Y. F. Zhang, G. D. chen, and J. W. Mi, "Disturbance-rejection high-precision motion control of a stewart platform," *IEEE Transactions on Control Systems Technology*, vol. 12, no. 3, pp. 364-374, 2004.

[32] Z. Gao, S. Hu, and F. Jiang, "A novel motion control design approach based on active disturbance rejection," *Proceedings of IEEE Conference on Decision and Control*, pp. 4877-4882, 2001.

[33] J. J. Gertler, "Survey of model-based failure detection and isolation in complex plants," *IEEE Control Systems Magazine*, vol. 8, no. 6, pp. 3-11, 1988.

[34] A. Radke and Z. Gao, "A survey of state and disturbance observers for practitioners," *Proceedings of the 2006 American Control Conference*, pp. 5183-5188, 2006.

[35] A. Tornambe and P. Valigi, "A Decentralized controller for the robust stabilization of a class of MIMO dynamical systems," *Journal of Dynamic Systems Measurement and Control*, vol. 116, pp. 293-304, 1994.

[36] S. Oh and H. K. Khalil, "Output feedback stabilization using variable structure control," *International Journal of Control*, vol. 62, no. 4, pp. 831-848, 1995.

[37] H. K. Khalil, "Nonlinear output-feedback tracking using high-gain observer and variable structure control," *Automatica*, vol. 33, no. 10, pp. 1845-1856, 1997.

[38] H. K. Khalil, *Nonlinear Systems,* Prentice Hall, 2002.

[39] L. B. Freidovich and H. K. Khalil, "Performance recovery of feedback-linearization-based designs," *IEEE Transactions on Automatic Control*, vol. 23, no. 10, pp. 2324-2334, 2008.

[40] F. Goforth,"On motion control design and tuning techniques," *Proceedings of the 2004 American Control Conference*, pp. 716-721, 2004.

[41] Q. Zheng and Z. Gao, "Motion control opmitimization: problem and solutions," *Interntional Journal of Intelligent control and systems*, vol. 10, no. 4, pp. 269-276, 2006.

[42] Y. Hou, Z. Gao, F. Jiang, and B. Boulter, "Active disturbance rejection control for web tension regulation," *Proceedings of the 40th IEEE Conference on Decision and Control*, pp. 4974-4979, 2001.

[43] B. Sun and Z. Gao, "A DSP-based active disturbance rejection control design for a 1KW H-bridge DC-DC power converter," *IEEE Trans. on Industrial Electronics*, vol. 52, no. 5, pp. 1271-1277, 2005.

[44] W. Zhou, S. Shao, and Z. Gao, "A stability study of active disturbance rejection control problem by a singular perturbation approach," *Applied Mathematical Sciences*, vol. 3, no. 10, pp. 491 - 508, 2009.

[45] Q. G. Wang, *Decoupling Control*, Springer, 2003.

[46] B. S. Morgan, "The synthesis of linear multivariable systems by state variable feedback," *IEEE Transactions on Automatic Control*, AC-9, pp. 404-411, 1964.

[47] B. S. Gilbert, 'The decoupling of multivariable systems by state feedback," *SIAM Journal on Control*, vol. 7, no. 1, pp. 50-63, 1969.

[48] A. S. Morse and W. A. Wonham, "Decoupling and pole assignment by dynamic compensation," *SIAM Journal on Control*, pp. 317-337, 1970.

[49] W. C. Williams and P. J. Antsaklis, 'A unifying approach to the decoupling of linear multivariable systems," *International Journal of Control*, vol. 44, pp. 181-201, 1986.

[50] J. Descusse, "Block noninteracting control with (non)regular static state feedback: a complete solution," *Automatica*, vol. 27, pp. 883-886, 1991.

[51] F. Zheng, Q. G. Wang and T. H. Lee, "On the design of multivariable PID controllers via LMI approach," *Automatica*, vol. 38, pp. 517-526, 2002.

[52] I. N. Voznesenskii, "On controlling machines with a large number of controlled parameters," *Avtomatika i Telemekhanica,* nos. 4-5, pp. 65-78, 1938.

[53] R. J. Kavanagh, "The multivariable problem," *Progress in Control Engineering*, vol. 3, pp. 94-12, 1966.

[54] H. S. Tsien, *Engineering Cybernetics*, McGraw-Hill, New York, 1954.

[55] P. L. Falb and W. A. Wolovich, "Decoupling in design and syntheis of multivariable systems," *IEEE Transactions on Automatic Control*, AC-12, pp. 651-669, 1967.

[56] W. A. Wonham and A. S. Morse, "Decoupling and pole assignment in linear multivariable systems: a geometric approach," *SIAM Journal on Control*, vol. 8, pp. 1-18, 1970.

[57] W. A. Wonham, *Linear Multivariable Control: A geometric approach*, 3rd edition, Springer, 1986.

[58] L. M. Silverman and H. J. Payne, "Input-output structure of linear systems with application to decoupling problem," *SIAM Journal on Control*, vol. 9, pp. 199-233, 1971.

[59] L. M. Silverman, "Inversion of multivariable linear systems," *IEEE Transactions on Automatic Control*, vol. 14, pp. 270-276, 1969.

[60] J. Descusse, J. F. Lafay and M. Malabre, "Solution to Morgan's problem," *IEEE Transactions on Automatic Control*, AC-33, pp. 732-739, 1988.

[61] C. Commault,, J. M. Dion and J. A. Torres, "Minimal structure in the block decoupling problem with stability," *Automatica*, vol. 27,pp. 331-338, 1991.

[62] C. A. Desoer and A. N. Gundes, "Decoupling linear multiinput multioutput plants by dynamic output feedback: An algebraic theory," *IEEE Transactions on Automatic Control*, vol. 31,pp. 744-750, 1986.

[63] M. L. J. Hautus and M. Heymann, "Linear feedback decoupling – transfer function analysis," *IEEE Transactions on Automatic Control*, vol. 28, pp. 823-832, 1983.

[64] T. G. Koussiouris, "A frequency domain approach to the block decoupling problem: I — The solvability of block decoupling problem by state feedback and a constant non-singular input transformation," *International Journal of Control*, vol. 29, pp. 911-1010, 1979.

[65] T. G. Koussiouris, "A frequency domain approach to the block decoupling problem: II — Pole placement while block-decoupling a minimal system by state feedback and a constant non-singular input transformationn," *International Journal of Control*, vol. 32, pp. 443-464, 1980.

[66] L. Pernebo, "An algebraic theory for the design of controllers for linear multivariable systems," *IEEE Transactions on Automatic Control*, vol. 26, pp. 171-193, 1981.

[67] C. A. Lin and T. F. Hsieh, "Decoupling controller design for linear multivariable plants," *IEEE Transactions on Automatic Control*, vol. 36, pp. 485-489, 1991.

[68] Y. Peng, "A general decoupling precompensator for linear multivariable systems with application to adaptive control," *IEEE Transactions on Automatic Control*, vol. 35, pp. 344-348, 1990.

[69] M. G. Safonov and B. S. Chen, "Multivaribale stability-margin optimization with decoupling and output regulation," *IEE Proceedings Part D*, vol. 129, pp. 276-282, 1982.

[70] A. I. G. Vardulakis, "Internal stabilization and decoupling in linear multivari-

able systems by unity output feedback compensation," *IEEE Transactions on Automatic Control*, AC-32, pp. 735-739, 1987.

[71] A. Linnemann and R. Maier, "Decoupling by precompensation while maintaining stabilizability," *Proceedings of the 29th IEEE Conference on Decision and Control*, pp. 2921-2922, 1990.

[72] Q.-G. Wang, "Decoupling with internal stability for unity output feedback systems," *Automatica*, vol. 28, pp. 411-415, 1992.

[73] A. Linnemann and Q.-G. Wang, "Block decoupling with stability by unity output feedback – Solution and performance limitations," *Automatica*, vol. 29, pp. 735-744, 1993.

[74] W.-T. Wu, Z.-P. Hwang, and Y.-L. Hsu, "Robust decoupling control based on external loops," *Chemical Engineering Communications*, vol. 169, pp. 25-35, 1998.

[75] A. Ito and M. Shiraishi, "Robust decoupling control for articulated robot," *JSME International Journal, Series C, Dynamics, Control, Robotics, Design and Manufacturing*, vol. 40, pp. 89-96, 1997.

[76] Q. Zheng, L. Q. Gao, and Z. Gao, "On Estimation of Plant Dynamics and Disturbance from Input-Output Data in Real Time," *Proceedings of the IEEE Multi-Conference on Systems & Control*, pp. 1167-1172, Singapore, October 1-3, 2007.

[77] Manual for Model 220 Industrial Emulator/Servo Trainer, http://www.mne.psu.edu/ray/me355web/IndustrialEmulator.pdf, Educational Control Products, 5725 Ostin Avenue, Woodland Hills, CA 91367, 1995.

[78] Q. Zheng, L. Q. Gao, and Z. Gao, "On Stability Analysis of Active Disturbance Rejection Control for Nonlinear Time-Varying Plants with Unknown Dynamics," *Proceedings of the 46th IEEE Conference on Decision and Control*, pp. 3501-3506, New Orleans, LA, USA, December 12-14, 2007.

[79] R. Bellman, *Introduction to Matrix Analysis*, RAND Corporation, New York, 1997.

[80] Q. Zheng, Z. Chen, and Z. Gao, "A Practical Dynamic Decoupling Control Approach," *Control Engineering Practice*, vol. 17, no. 9, pp. 1016-1025, 2009.

[81] Y. Huang, K. Xu, J. Han, and J. Lam, "Flight Control Design Using Extended State Observer and Non- Smooth Feedback," *Proceedings of the 40th IEEE Conference on Decision and Control*, pp. 223-228, 2001.

[82] R. Miklosovic and Z. Gao, "A Dynamic Decoupling Method for Controlling High Performance Turbofan Engine," *Proceedings of the 16th IFAC World Congress*, 2005.

[83] B. Yao, M. Al-Majed, and M. Tomizuka, "High-performance robust motion control of machine tools: An adaptive robust control approach and comparative experiments," *IEEE/ASME Transaction on Mechatron.*, vol. 2, pp. 63-76, 1997.

[84] B.-K. Choi, C.-H. Choi, and H. Lim, 'Model-based disturbance attenuation for CNC machining centers in cutting process," *IEEE/ASME Transaction on Mechatron.*, vol. 4, pp. 157-168, 1999.

[85] B. S. Dayal and J.F. MacGregor, "Recursive exponentially weighted PLS and its application to adaptive control and prediction," *Journal of Process Control*, vol. 7, no. 3, pp. 169-179, 1997.

[86] Q. Zheng, L. Dong, and Z. Gao, "Control and Rotation Rate Estimation of Vibrational MEMS Gyroscopes," *Proceedings of the IEEE Multi-Conference on Systems & Control*, pp. 118-123, Singapore, October 1-3, 2007.

[87] B. Roffel and B. H. Betlem, *Advanced Practical Process Control*, Springer, 2004.

[88] S. Park and R. Horowitz, "Adaptive Control for Z-axis MEMS Gyroscopes," *Proceedings of American Control Conference*, pp. 1223-1228, 2001.

[89] Y. Yazdi, F. Ayazi, and K. Najafi, "Micromachined inertial sensors," *Proceedings of the IEEE*, vol. 86, no. 8, pp. 1640-1659, 1998.

[90] R. Leland, "Lyapunov based adaptive control of a MEMS gyroscope," *Proceedings of American Control Conference*, pp. 3765-3770, 2002.

[91] R. P. Leland, Y. Lipkin, and A. Highsmith, "Adaptive oscillator control for a vibrational gyroscope," *Proceedings of American Control Conference*, pp. 3347-3352, 2003.

[92] S. Park, *Adaptive control strategies for MEMS gyroscopes*, PhD Dissertation, The University of California Berkeley, 2000.

[93] A. M. Shkel, R. Horowitz, A. A. Seshia, S. Park, and R. T. Howe, "Dynamicsw and control of micromachined gyroscopes," *Proceedings of American Control Conference*, pp. 2119-2124, 1999.

[94] S. Park and R. Horowitz, "Adaptive control for the conventional mode of operation of MEMS gyroscopes," *Journal of Microelectromechanical Systems*, vol. 12, no. 1, pp. 101-108, 2003.

[95] J. D. John and T. Vinay, "Novel concept of a single-mass adaptively controlled

triaxial angular rate sensor," *IEEE Sensors Journal*, vol. 6, no. 3, pp. 588-595, 2006.

[96] R. M'Closkey, S. Gibson, and J. Hul, "System identification of a MEMS gyroscope," *Journal of Dynamic Systems, Measurement, and Control*, vol. 123, pp. 201-210, 2001.

[97] M. Salah, M. McIntyre, D. Dawson, and J. Wagner, "Time-varying angular rate sensing for a MEMS Z-axis gyroscope," *Proceedings of the 45th IEEE Conference on Decision and Control*, pp. 2165-2170, 2006.

[98] W. A. Clark, R. T. Howe, and R. Horowitz, "Surface micromachined Z-axis vibratory rate gyroscope," *Tech. Dig. Solid-State Sensor and Actuator Workshop*, pp. 283-287, 1996.

[99] L. Dong, Q. Zheng, and Z. Gao, "On Control System Design for the Conventional Mode of Operation of Vibrational Gyroscopes," *IEEE Sensors Journal*, vol. 8, no. 11, pp. 1871-1878, 2008.

[100] Q. Zheng, L. Dong, D. H. Lee, and Z. Gao, "Active Disturbance Rejection Control for MEMS gyroscopes," *Proceedings of the American Control Conference*, pp. 4425-4430, Seattle, Washington, USA, June 11-13, 2008.

[101] Q. Zheng, L. Dong, D. H. Lee, and Z. Gao, "Active Disturbance Rejection Control and Implementation for MEMS Gyroscopes," to appear, *IEEE Transactions on Control System Technology*, 2009.